Simulation Of The Internal Flow Characteristic Of Diesel Injector Using CFD Software

by

MOHD FAISAL BIN HUSIRAN

DISSERTATION

Submitted to the Mechanical Engineering Programme

in Partial Fulfillment of the Requirements

for the Degree

Bachelor of Engineering (Hons)

(Mechanical Engineering)

June 2004

Universiti Teknologi PETRONAS

Bandar Seri Iskandar

31750 Tronoh

Perak Darul Ridzuan

t

TJ

795

.m 697

2004

1. Diesel motor

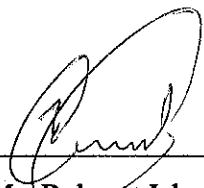2. ME -- Thesis

CERTIFICATION OF APPROVAL

Simulation of the Internal Flow Characteristic of Diesel Injector Using CFD Software

By

Mohd Faisal Bin Husiran

A project dissertation submitted to the

Mechanical Engineering Programme

Universiti Teknologi PETRONAS

in Partial Fulfillment of the Requirements for the

BACHELOR OF ENGINEERING (Hons)

(MECHANICAL ENGINEERING)

Approved by,

(Mr. Rahmat Iskandar)

UNIVERSITI TEKNOLOGI PETRONAS

TRONOH, PERAK

May 2004

CERTIFICATION OF ORIGINALITY

This is to certify that I am responsible for the work submitted in this project, that the original work is my own except as specified in the references and acknowledgements, and that the original work contained herein have not been undertaken or done by unspecified sources or persons.

MOHD FAISAL BIN HUSIRAN

ABSTRACT

Fuel injectors deliver fuel to cylinders of internal combustion (IC) engines. The fuel is sprayed through an injector nozzle, typically at high pressure, to improve the mixing of fuel with air and increase the combustion efficiency. Modern passenger cars and trucks use higher injection pressures than earlier models to improve the atomization of fuel in order to reduce the emission levels of IC engines. Unfortunately, high operating pressures in diesel injectors can cause cavitation in the liquid fuel, leading to degradation in performance and structural damage to the injector. Because fuel injectors are typically small, experimental measurements of this phenomenon are difficult to make, so analysis through CFD is an appealing alternative.

The project scope is mainly on the comparing the simulation results with experimental data (using a scaled up model). In particular, it is of interest to study the flow behaviour especially in determining the cavitation and atomization using CFD software, ANSYS 6.0. The methodology of project work consists of literature review, Gantt chart and simulation.

The main objective of this project is to do simulation on internal flow of diesel fuel injector using ANSYS, then comparing and analysing the results for both experiment and simulation. Interpretation from the simulation results lead to the better explanation for the cavitation and atomisation phenomena. Finally, at the end of this project the computational cost can be reduced by the simplification of simulation process.

The simulations cover on the single-phase and 2 dimensional analyses which focus on the effect of the sharp and blunt inlet nozzle to the cavitation flow. Meanwhile, for the atomization and hydraulic flip flow, volume fraction analysis will be the best method to express the atomization flow as explain in the chapter 2. As conclusion for this project, ANSYS software is reliable to simulate the internal fluid flow problems and able to produce a quite accurate outcome (with some limitation) to assist in further study on the internal fluid flow behaviour.

ACKNOWLEDGEMENT

NOMENCLATURE

A   effective flow area through the contraction

A_c nominal nozzle area

P_1 absolute upstream pressure i.e. injection pressure

P_2 absolute downstream pressure i.e. reservoir pressure

P_V vapour pressure of fluid in the nozzle

C_V cavitation number

Re Reynolds number

ρ fluid density

μ_L dynamic viscosity of fluid

σ surface tension

TABLE OF CONTENT

LIST OF FIGURE

LIST OF TABLE

LIST OF APPENDIX

CHAPTER 1

INTRODUCTION

The design of modern diesel fuel injectors to an operating pressure of approximately 20 atmospheres is driven by the emission requirements. Cavitation of the fuel inside the injector orifices has long been known to occur because of the structural damage to the orifices. The exact internal flow behaviour of the injector is not yet perfectly understood since the size of the injector itself is very small. Therefore, by aid of the CFD software will help determine the flow characteristic of the injector.

Two main factors that will be emphasized in this project are cavitation and atomisation effect. Flow cavitation is considered a major problem affecting performance of high-pressure diesel injectors (1). The cavitating flow is a two-phase flow by nature with gaseous phase generally dispersed within the liquid phase in the form of minute bubbles.

1.1   Background of Study

A diesel engine is different relative to a gasoline engine by its operation. In the combustion chamber the ignition of the diesel engine is only by compression. Therefore it is good to have the injector produce a very heterogeneous mixture of liquid droplets, fuel vapour mixed with air, and some air pockets all-present at the same time. This is to ensure that the fuel will burn rapidly in the premixed mode immediately after ignition.

In general, this project aims to simulate the internal flow of diesel fuel injector. The simulation will help to monitor the flow characteristic of the injector in detail. Therefore, validation and comparison of the simulation results with the experimental data are very

essential. The outcome of this analysis can be used for the improvement of the fuel injector design.

1.2   Problem Statement

1.2.1   Problem identification

Currently the performance of diesel fuel injector can be gauged easily from the output. But the internal flow characteristic that drive the output flow behaviour is not yet perfectly understood since a very small size of injector (approximately 150 μm). Therefore, the scaled up model is used in order to analyse the system. This project focuses on the simulation to compare the results with experimental data and study in details on the flow characteristic.

1.2.2   Significant of the project

The injector is an essential part of the diesel engine. Currently, many research (1-2) have been done to improve the injector performance. So, by the simulation, the flow characteristic will be studied further especially for the steady state case as well as transient case. This project will expose the student on the principle and the behaviour of the injector flow using CFD software simulation. The information from this project hopefully can help to design the flow pattern and can be used for other applications. The outcome of this project is very promising in future development of fuel injector.

1.3   Objectives

- The main objective of this project is to do a simulation on the internal flow of scaled up-diesel injector rig using the CFD software.
- To compare and analyse the results of the experiment and the simulation.
- To observe the flow characteristic differences between sharp inlet nozzle and blunt inlet nozzle.

- To reduce the computational cost for the simulation. The time taken for the simulation is very long (almost 5 hours for transient case) for fine mesh. Therefore, an adequate number of elements for mesh are set to reduce the simulation time.

- To study the internal flow for steady state case with plan to look further at transient case.

1.4   Scope of Study

The project requires understanding of the principal and the behaviour of diesel fuel injector especially on the internal flow characteristic. The important factors on this project are the steady state flow, cavitation concept and the atomisation during the process flow. The simulation must be in the 2-phase mode (gas and liquid) in order to make a comparison with the results obtained from the simulation and the experimental data.

For the first part of the project, literature review on the injector and simulation of single phase condition for finding the adequate meshing, to reduce the computational cost were covered. The second part of the project focused on the 2-phase simulation which is estimated to be the exact flow inside the injector. The entire dimension and the other parameters used in the simulation process follow as per scaled up diesel injector experiment. This is very important to make sure that the simulation and experimental results have been compared using the same model, for dynamic similarity. The project looks at the steady state cases and also has the transient case analysis.

CHAPTER 2

LITERATURE REVIEW & THEORY

2.1   Cavitation

Cavitation bubbles form because of the mechanical force (very low static pressure) that occurs in high-speed nozzle flow near a sharp inlet corner (2). This low static pressure is predicted by incompressible potential flow theory, which indicates that flow around a sharp corner will have infinite negative pressure. The sharper the corner and the higher the velocity, the more likely cavitation is to occur.
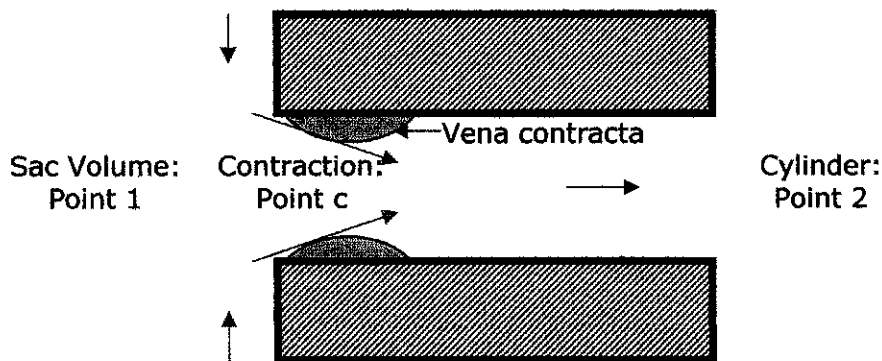
Figure 2.1: Schematic of nozzle flow (2)

In the case of a sharp inlet, where the flow separates at the corner, the flow experiences a vena contracta (2). Vena contracta is the area which the sudden pressure drop in flow will occur. At this area, the cavitation flow will suspected to happen. Cavitation is the sudden formation and collapse of bubbles in a fluid cause by mechanical force, which is pressure. This is due to pressure drop below atmospheric pressure. Point 1 would be downstream of the injector needle that the local velocity would be small, such as in the sac of the

injector. Point c is downstream of the inlet, where the vena contracta effect is a maximum. The coefficient of contraction, C_c, is defined:

$$C_C = \frac{A_C}{A}$$

[2.1]

Another relevant integral property of the flow is the coefficient of discharge, C_d. The coefficient of discharge represents the efficiency of the nozzle between points 1 and 2 and thus is a measure of any losses occurs in the nozzle. The definition of the coefficient of discharge, C_d is:

$$C_d = \frac{\dot{M}}{A\sqrt{2\rho(P_1 - P_2)}}$$

[2.2]

The definition of C_d, continuity, and Bernoulli's equation are combined to obtain the following expression for the coefficient of discharge of a cavitating nozzle, C_D:

$$C_D = C_C \left(\frac{P_1 - P_V}{P_1 - P_2}\right)^{\frac{1}{2}}$$

[2.3]

The pressure ratio in the right side of equation above turns out to be a very useful cavitation parameter and is referred to as K in the remainder of this paper.

$$K = \frac{P_1 - P_V}{P_1 - P_2}$$

[2.3]

In an actual injector, P_1 represents the sac pressure. Unfortunately, it is extremely difficult to measure the sac pressure of a working injector. Instead, fuel injectors may be equipped with a pressure transducer just *upstream* of the needle. Because the exact sac pressure is not known, the coefficient of discharge will actually include strong needle effects. During periods of low needle lift, most likely a large pressure loss across the needle would happen. For the beginning and the ending portions of the injection, the

needle will dominate the behaviour of the coefficient of discharge. Due to needle effects, the measured value of K is only credible during large needle lift. For this reason, the bulk of the previous analysis should be applied to the portion of injection where the needle is nearly fully open.

2.2   Atomisation

The fuel jet forms a cone-shaped spray at the nozzle exit under typical diesel engine injection conditions. This behaviour is called atomisation backup regime, and it produces droplets with sizes very much less than the nozzle exit diameter (1). This behaviour is different from other modes of liquid jet breakup. At low velocity, breakup is due to the unstable growth of surface waves caused by surface tension and results in drops larger than jet diameter. As jet velocity is increased, forces due to the relative motion of the jet and the surrounding air augment the surface tension force and lead the drops sizes of the order of the jet diameter. In diesel engine, the distribution of fuel into smaller droplets allow for better combustion. A good combustion hopefully improved efficiency and reduced emissions

Cavitation is also a possible contributor of atomisation. In nozzle flow behaviour, the recirculating region causes the effective area of flow to reduce. The flow will then reduce the pressure and increase the amount of radial vorticity in the fluid. This assists atomisation of the fluid as it emerges from the confines of the nozzle walls.

The generation and collapse of these bubbles is said to introduce increased levels of turbulence and hence the greater atomisation effect will happen. The quality of atomisation increases with increasing injection pressure up to a threshold value. Over this value, the flow emerges in a condition known as hydraulic flip. Hydraulic flip is the condition where the high velocity flow happens. The fluid is not being contact with nozzle wall after the flow separates at the corner. The output flow from the injector will be very smooth and glass-like shape. The hydraulic flip flow occurs because of high

6

pressure different between the inlet and outlet. This pressure different will lead to high flow velocity. Moreover the flow does not have any droplets or bubbles generation.

2.3 Computational Fluid Dynamic (CFD) Software - ANSYS

This project used ANSYS 6.0 to simulate all the models and cases to accomplish the results as stated in the objectives. ANSYS is finite element analysis software that enables users to perform several tasks. The ANSYS programme has a comprehensive graphical user interface (GUI) that gives users easy, interactive access to programme functions, commands, documentation, and reference material. An intuitive menu system helps users navigate through the ANSYS programme. Users can input data using a mouse, a keyboard, or a combination of both. (3)

2.3.1 Overview of FLOTRAN Analysis

A typical FLOTRAN analysis consists of seven main steps:

1. Determine the problem domain.
2. Determine the flow regime.
3. Create the finite element mesh.
4. Apply boundary conditions.
5. Set FLOTRAN analysis parameters.
6. Solve the problem.
7. Examine the results.

2.3.2 Characteristics of the FLOTRAN Elements

The ANSYS FLOTRAN elements used in this simulation, FLUID141, can solve for two-dimensional flow, pressure, and temperature distributions in a single phase viscous fluid. For these elements, the ANSYS programme calculates velocity components, pressure, and temperature from the conservation of three properties: mass, momentum, and energy (3).

7

The FLUID141 element has these characteristics:

Dimensions: 2-Dimensional

Shape: Quadrilateral, four nodes or triangle, three nodes

Degrees of freedom: Fluid velocity, pressure, temperature, turbulent kinetic energy, turbulent energy dissipation, multiple species mass fractions for up to six fluids.

Other features of the FLOTRAN elements include:

- A two-equation turbulence model for simulating turbulent flows.
- Derived results, such as Mach number, pressure coefficient, total pressure, shear stress, y plus at walls, and stream function for fluid analyses and heat flux and heat transfer (film) coefficient for thermal analyses.
- Fluid boundary conditions, including velocities, pressures, and the turbulence quantities kinetic energy and kinetic energy dissipation rate.
- Thermal boundary conditions, including temperature, heat flux, volumetric heat sources, and heat transfer (film) coefficient.

ANSYS can solve problems in Cartesian, cylindrical, polar, and axisymmetric coordinate systems. If a problem is axisymmetric, activating a swirl option allows user to calculate a velocity component normal to the axisymmetric plane.

2.3.3 Turbulent flow

Flows are classified as laminar or turbulent. For any flow geometry, there is one (or more) dimensionless parameter such that with this parameter value below a particular value, the flow is laminar. While with the parameter value larger than certain value, it is turbulent. For pipe flow this parameter is the Reynolds number. The value of the Reynolds number must be less than approximately 2100 for laminar flow and greater than approximately 4000 for turbulent flow.

The dimensionless Reynolds number measures the ratio of inertial and viscous forces to help determine whether or not the turbulence model should be activated in the ANSYS

8

simulation. The Reynolds number (*Re*) is defined in terms of the properties of the fluid, a characteristic velocity, and a characteristic dimension (3):

$$\text{Re} = \frac{\rho V L_C}{\mu}$$

The density (mass/length^3) and absolute viscosity μ (mass/length-time) are properties of the fluid. For internal flow problems, the characteristic dimension is the hydraulic diameter, defined as:

$$L_c = D_h = \frac{4(\text{cross - sectional Flow Area})}{\text{Wetted Perimeter}}$$

2.3.4 Turbulence Model

The distinction between laminar and turbulent flow lies in the ratio of the inertial transport to the viscous transport. As this ratio increases, instabilities develop and velocity fluctuations begin to occur. A turbulence model accounts for the effect of these fluctuations on the mean flow by using an increased viscosity (the effective viscosity) in the governing equations. The effective viscosity is the sum of the laminar viscosity (which is a property of the fluid) and turbulent viscosity (which is calculated from a turbulence model).

$$\mu_e = \mu_{laminar} + \mu_{turbulence}$$

Generally, the more turbulent the flow field, the higher the effective viscosity. ANSYS FLOTRAN offers six turbulence models (3):

1. Standard k-epsilon Model
2. Zero Equation Turbulence Model (ZeroEq)
3. Re-Normalized Group Turbulence Model (RNG)
4. K-epsilon Model due to Shih (NKE)
5. Non-linear Model of Girimaji (GIR)
6. Shih, Zhu, Lumley Model (SZL)

The details for each models are explain in the **Appendix 2.1**.

CHAPTER 3
EXPERIMENT DETAILS

3.1   Introduction

The experimental data is basically used to verify the CFD simulation. This project mainly focuses on providing the CFD data as comparison to the results of Dalli (5). Y.Laoonual et. al. also did quite similar experiment and equipment (6), which is both of the experiments data are used as the baseline comparison for this project. In this chapter, only the essential information from the experiment is included.

3.2   Experiment Details

3.2.1   Experimental Apparatus

A schematic diagram on the experimental apparatus used for the study of VCO nozzles is shown in **Figure 3.1** (6). The apparatus consists of three main parts: The high pressure rig, the scaled up nozzle and the auxiliary equipment. In the high pressure rig the working fluid (water) is pressurized in a reservoir up to a maximum working pressure of 5MPa using nitrogen gas. The nozzle; made from Perspex is contained in the injector body. Flow through the nozzle is controlled by the nozzle valve, which has a piece of rubber inserted at the bottom to provide an adequate seal in the closed position. To instigate injection the cam lever arm is moved rapidly (with a repetitive dynamic action) by the action from the piston rod of a linear compressed air actuator, via a solenoid valve, operated by a control switch. Once the cam lever arm move, the valve is moved up and injection into atmospheric condition begins.
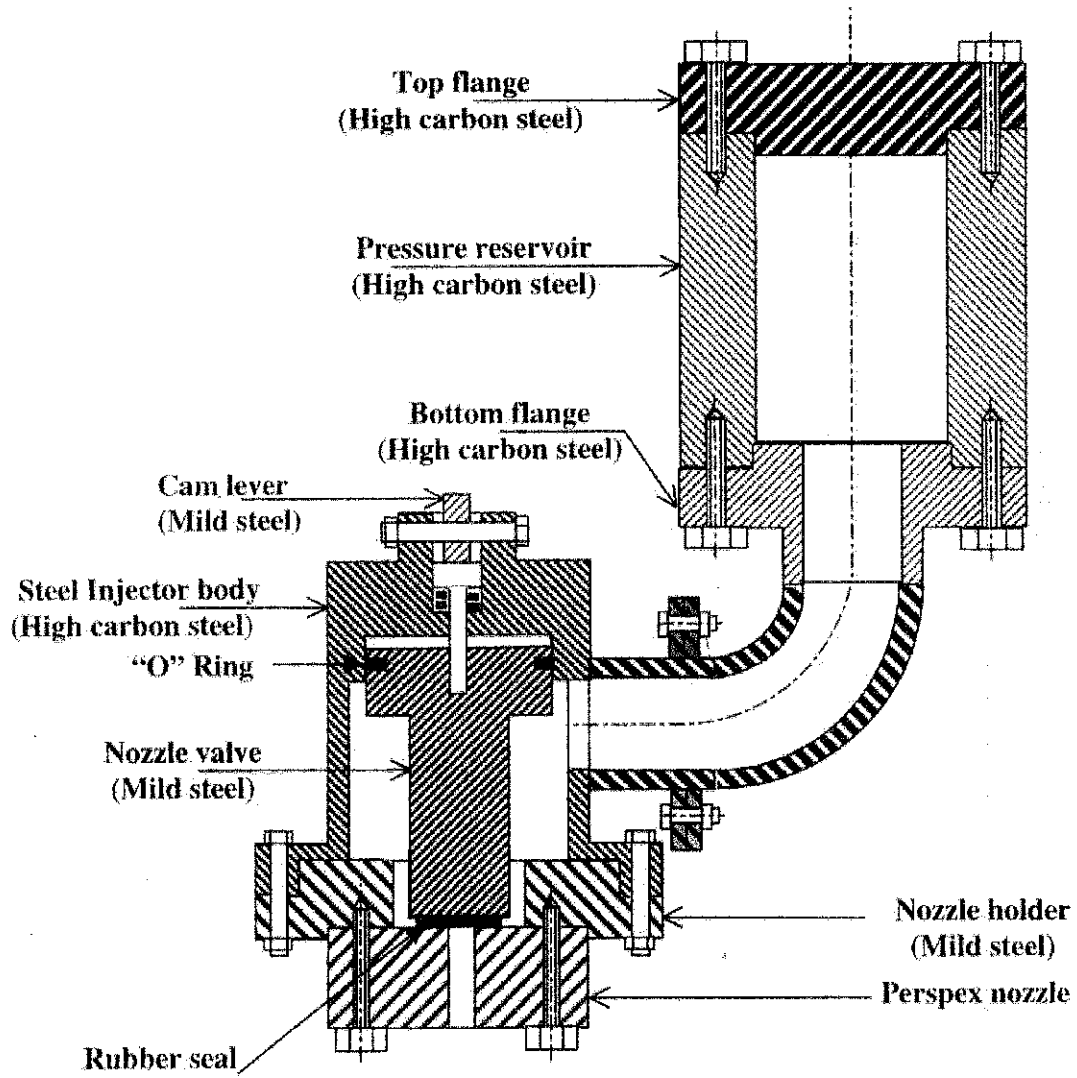
Figure 3.1: Assembly drawing of injector apparatus (5)

The details dimensions for both shapes of the experimental scaled up diesel injector and the valve are shown in **Figure 3.2**, **Figure 3.3** and **Figure 3.4**.

11

PLAN VIEW

"O" Ring groove 2mm
deep, 4mm wide, I.D 92

10X10.5 dia holes

Φ 140

A   A

120°

P.C.D 116

Φ 80

86

SIDE VIEW

"O" Ring

10 – Holes
for M10 tap

50.4   30   Ø12

Ø16   11

39.6

Extension piece (Perspex)

DIMENSIONS IN mm
NOT TO SCALE
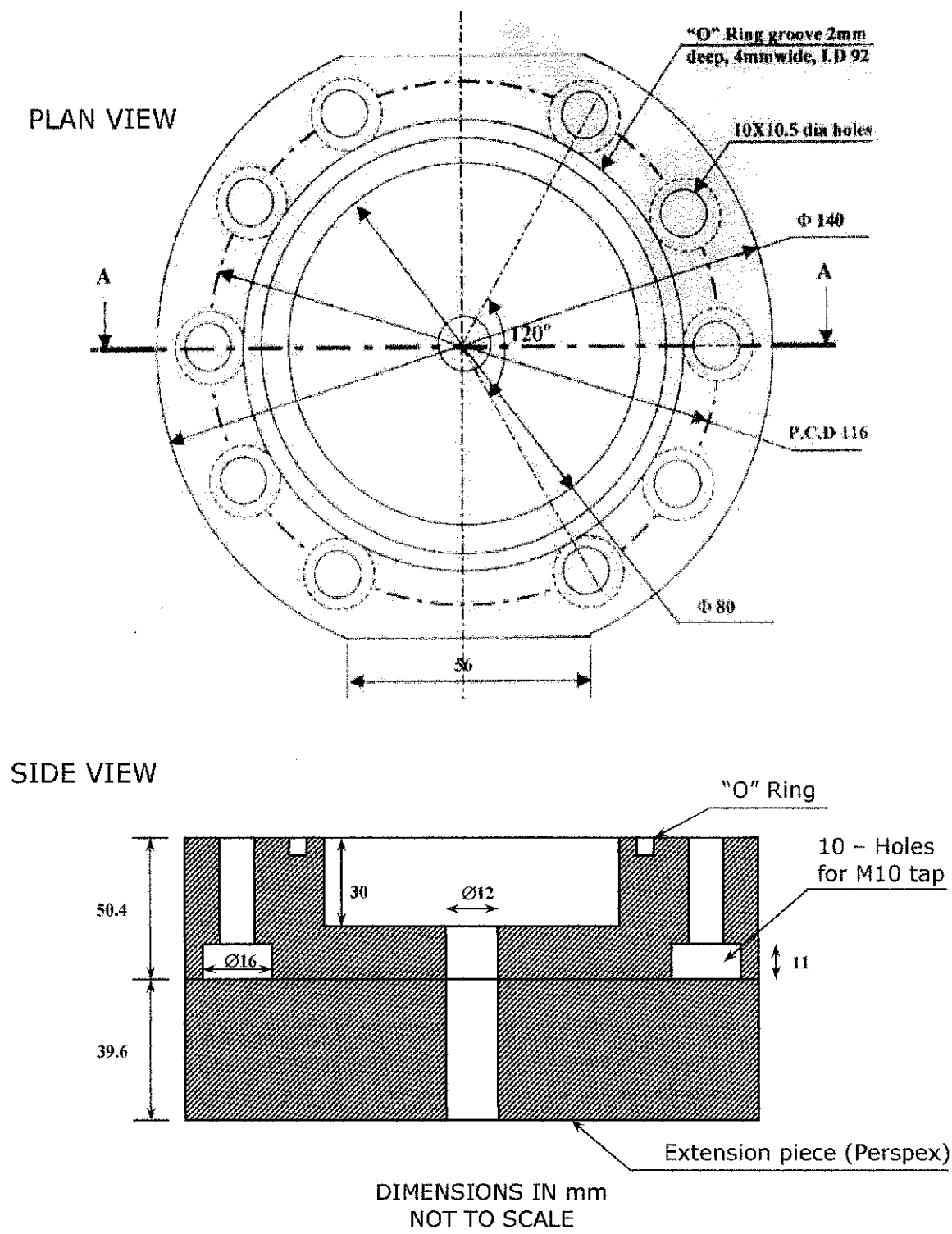
Figure 3.2: The 12 mm sharp inlet Perspex nozzle with the extension piece, L/d = 5 (5)

SIDE VIEW

"O" Ring groove

10 – Holes for M10 tap head

50.4

30

R=3

Ø16

11

39.6

Ø12

Extension piece (Perspex)

DIMENSIONS IN mm
NOT TO SCALE
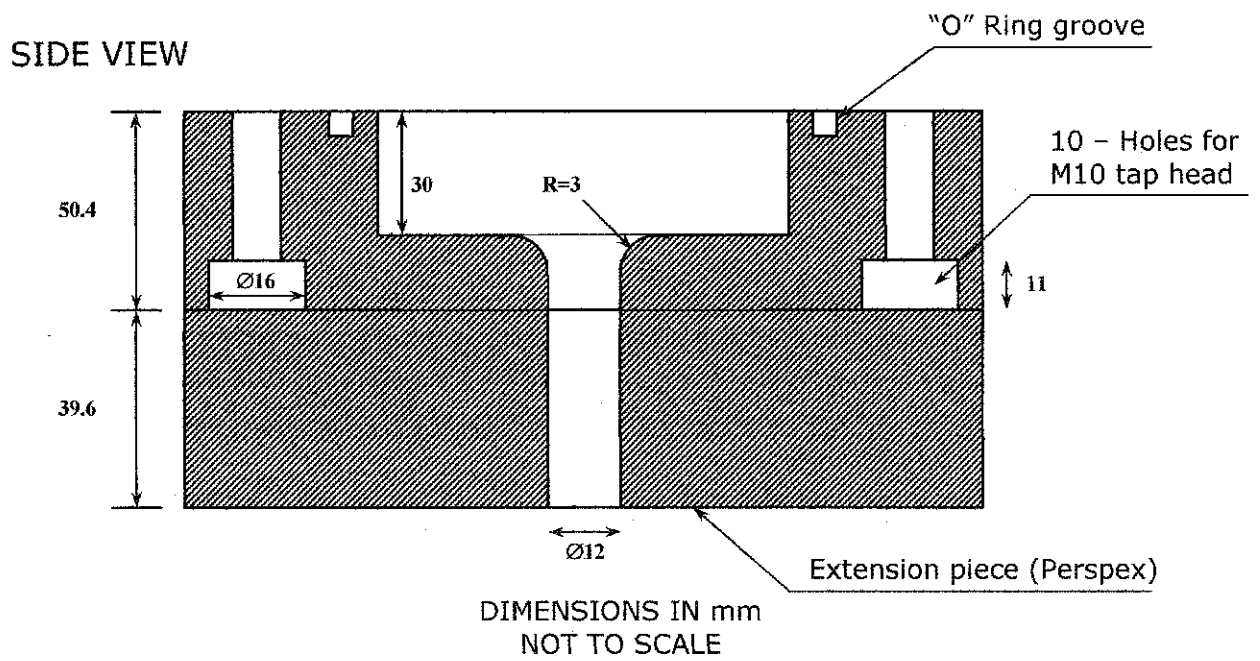
Figure 3.3: The 12 mm round inlet Perspex nozzle with the extension piece, L/d = 5 (5)

Ø 60

DIMENSIONS IN mm
NOT TO SCALE
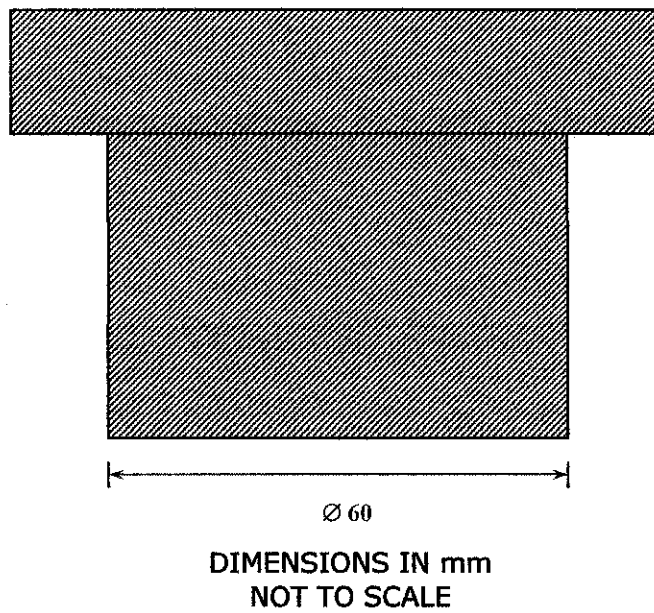
Figure 3.4: Nozzle valve (mild steel) (5)

13

3.2.2 Dimensionless Parameter

Several parameters are used in this experiment, and they are as described in the **Table 3.1**.

Liquid	Liquid density ρ_L Kg/m^3	Viscosity, μ_L N.s/m^2	P_V N/m^2	Surface tension σ N/m	δP bar	Fluid Velocity (m/s)	Reynolds number (Re)	Cavitation number (C$_V$)
Water	998	1.002E-3	2338	0.0727	1.70	18.57	2.22E+5	1.74
					2.72	23.52	2.81E+5	2.79
					4.76	31.11	3.72E+5	4.88
					6.80	37.16	4.44E+5	6.96
					13.61	52.55	6.28E+5	13.92
					19.74	63.31	7.57E+5	20.20
Diesel	850.6	2.676E-3	300	0.028	1.70	20.11	7.67E+4	1.70
					2.72	25.47	9.72E+4	2.73
					4.73	33.70	1.29E+5	4.78
					6.80	40.25	1.54E+5	6.82
					13.61	56.92	2.17E+5	13.64
					19.74	68.58	2.62E+5	19.80
Diesel fuel orifice, P1 = 1000 bar, Cd = 0.6, ρ_m = 23 kg/m3, P2 = 60 bar					960	285	1.36E+4	16

Table 3.1: The liquid used in experiments and typical values of dimensionless groups for 12 mm sharp inlet nozzle (5)

3.2.3 Experimental Results

The experiment of transient cavitation and separation in scaled-up model of VCO orifice by A.M. Dalli and also by Y.Laoonual et. al. shows the flow behaviour at the outlet of the nozzle are varies for different inlet pressure. They are two types of flow for the sharp inlet nozzle, which are the cavitating flow and the hydraulic flip flow (see **Figure 3.5**). The range for the cavitating flow is up to 25 psi inlet pressure. Once the value of the flow exceeds the range, the flow becomes hydraulic flip. **Table 3.2** (Dalli's results) and **Table 3.3** (the Y. Laoonual et. al.'s results) show the experimental findings using a pure water.

14

Pressure (psi)	Pressure (Pa)	Remarks
15	103421	Slight cavitation
25	172369	Severe cavitation
26	179264	Hydraulic flip
30	206843	Hydraulic flip
40	275790	Hydraulic flip
70	482633	Hydraulic flip
80	551581	Hydraulic flip
100	689476	Hydraulic flip
200	1378950	Hydraulic flip
290	1999480	Hydraulic flip

Table 3.2: Experimental results for sharp inlet nozzle (L/D = 5) by Dalli.

Phenomena	Model 1 : Plain nozzle			Model 2 : Round nozzle, r = 3		
	L/D	Pressure (gauge)		L/D	Pressure (gauge)	
		psi	MPa		psi	MPa
Incipient cavitation	5	20	0.138	5	20	0.138
	10	20	0.138	10	20	0.138
Super cavitation	5	25	0.172	5	30	0.207
	10	30	0.207	10	35	0.241
Total hydraulic flip	5	25	0.172	5	30	0.207
	10	30	0.207	10	*	*

Table 3.3: Experimental results by Y.Laoonual et. al. (6)

Slight / incipient cavitation   Severe / supercavitation   Hydraulic flip
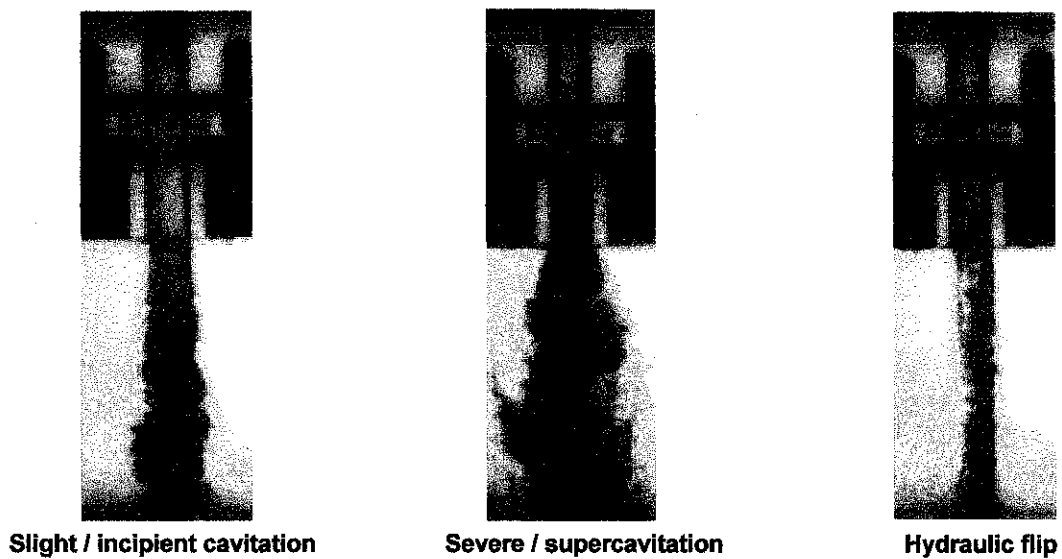
Figure 3.5: The principle flow regime taken by Y.Laoonual et. al.

CHAPTER 4

METHODOLOGY/PROJECT WORK

4.1 Literature Review

Literature review is important as the basic knowledge on diesel fuel injector concept need to be mastered. Books, journals and articles have to be referred from the library and the internet surfing had been done in order to have better understanding about this project.

4.2 Gantt Chart

The chart is used to monitor project progress. The project is divided into two semesters and there are several milestones to be completed (4). (**Appendix 4.1** and **Appendix 4.2**)

4.3 Simulation Using ANSYS

Simulation will be done on the single phase and the steady state case for blunt inlet injector. The nozzles are at 30 percent opening mode which the injector will lift up almost one third of the allowable limit. The solution can be further analysed for blunt inlet and transient case. The simulation is done according to the following steps:

Step 1 : Model generation – The drawing of the diesel injector will be generated.

Step 2 : Meshing – to analyse the model for each small nodes.

Step 3 : Key in required information, such as density of the fluid and other design parameters.

Step 4 : Setting up the boundary layer condition.

Step 5 : Simulate and getting the results.

Step 6 : Results comparing especially on flow characteristic.
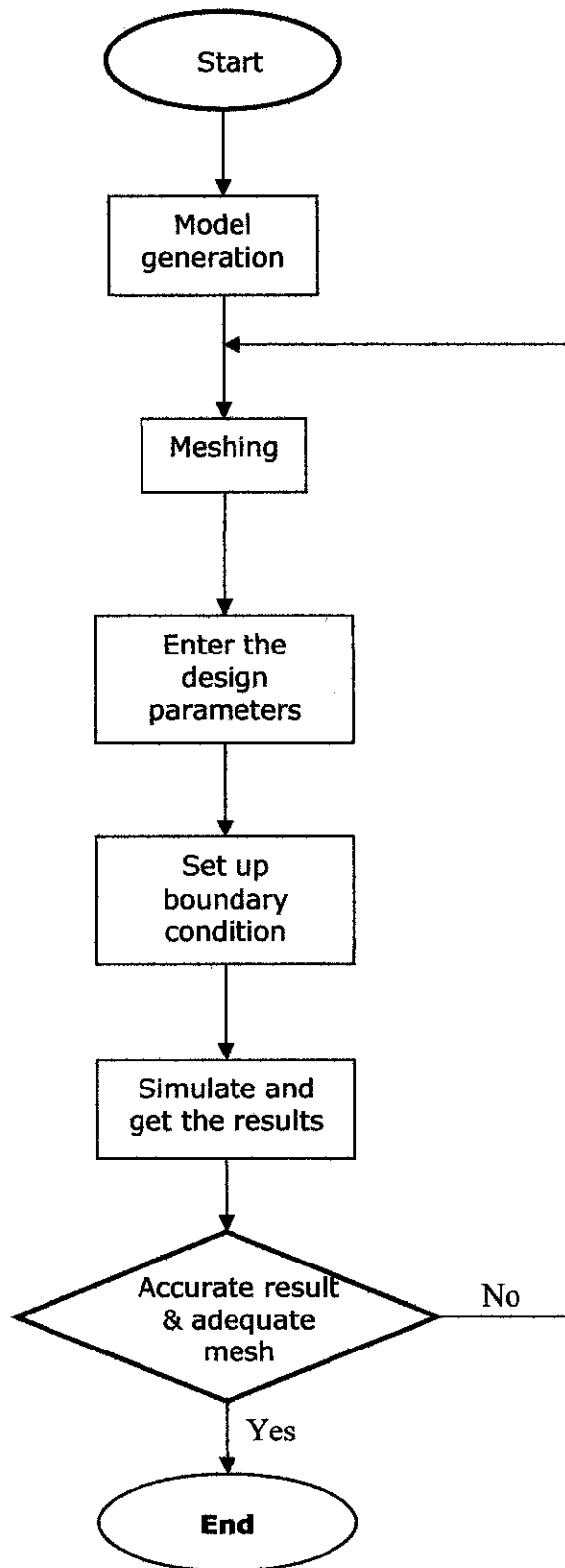
Figure 4.1: Simulation flowchart

4.4   Tools and Equipment

The project is completed with the aid of CFD software which is ANSYS. ANSYS finite element analysis, appropriate software enables users to perform the fluid simulation tasks. The ANSYS programme has a comprehensive graphical user interface (GUI) that gives users easy, interactive access to programme functions, commands, documentation, and reference material. An intuitive menu system helps users navigate through the ANSYS programme. Users can input data using a mouse, a keyboard, or a combination of both. For 2-phase analysis, ANSYS FLOTRAN had been used. The details about this software are discussed in the next chapter.

All simulation work for this project is done using a Pentium 4 computer with 256 MB RAM, 20 GB hard disk capacity and operational speed of 1.7 GHz. The computer uses Windows XP Professional as the operating system. Extra fan is needed because of the heat generated due to continuous running of the hard disk during the simulation.

CHAPTER 5

CFD MODELLING OF INTERNAL FLOW OF SCALED-UP DIESEL INJECTOR

5.1   Introduction

ANSYS consists of several simulation types. For this project, the internal flow characteristic evaluation, the ANSYS FLOTRAN was selected. The FLOTRAN CFD (Computational Fluid Dynamics) option to the other ANSYS products provide comprehensive tools for analyzing two-dimensional and three-dimensional fluid flow fields.

ANSYS FLOTRAN can perform several types of analysis; laminar or turbulent, thermal or adiabatic, free surface, compressible or incompressible, Newtonian or non-Newtonian and multiple species transport. These types of analyses are *not* mutually exclusive. For example, a laminar analysis can be thermal or adiabatic. A turbulent analysis can be compressible or incompressible.

The ANSYS FLOTRAN elements, FLUID141 and FLUID142, solve for two- and three-dimensional flow respectively, pressure, and temperature distributions in a single phase viscous fluid. For these elements, the ANSYS programme calculates velocity components, pressure, and temperature from the conservation of three properties: mass, momentum, and energy.

5.2 Basic drawing

The diagram below shows the basic drawing of 2-D model of scaled-up diesel injector. The needle valve is opened at 1:3 opening ratio (see **Figure 5.1**)

DIMENSIONS IN mm
NOT TO SCALE
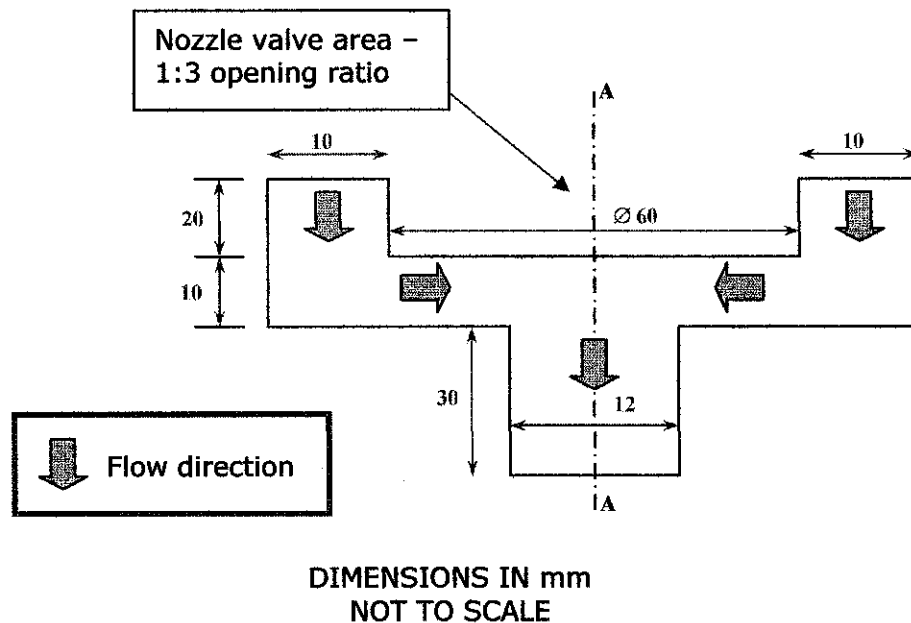
Figure 5.1: Basic drawing for the simulation

Since the axisymmetric model is used in ANSYS, the simulation will be done for one part of the injector. As example, the injector consists of $360°$ cylinder model and the centre of the cylinder is at the line A-A (refer **Figure 5.1**), ANSYS simulation only calculates one degree or one part of it. It means that, the calculation only base on the one portion of flow area with respect to centre line. The rest are assumed similar in flow pattern. The cutting line A-A, in the figure above also shows the symmetric line of the simulation drawing. In the 'axisymmetric theorem' (3), it mentions that the flow velocity at symmetric line will be perpendicular with the axis will equal to zero. This condition must be set up in the boundary condition in the software.

20

5.3 Specification of boundary condition and meshing concentration.

5.3.1 Boundary condition

Before continuing with the analysis, the boundary condition must be set up. The boundary condition will remain the same for any set of meshing. **Figure 5.2** can be referred for clear illustration.
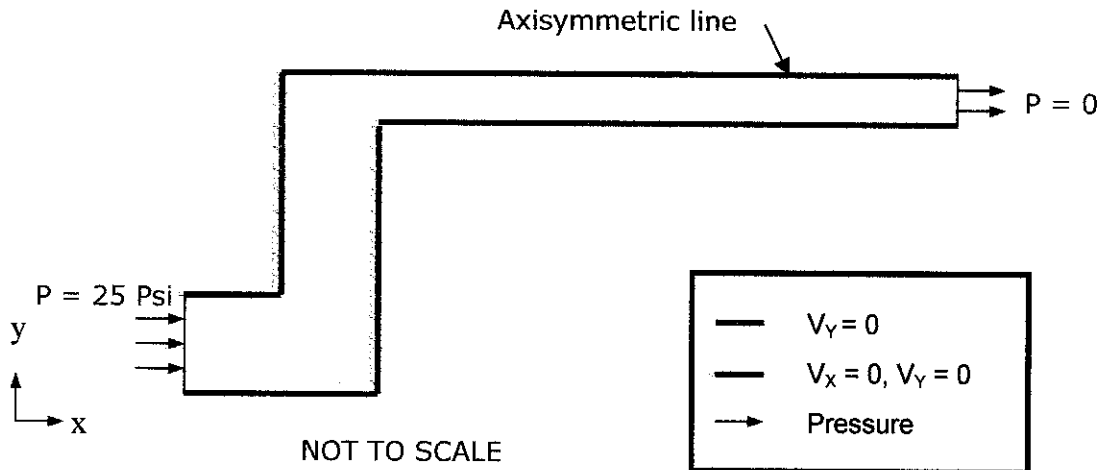
Figure 5.2: Boundary condition.

Specification of each parameter as shown in **Figure 5.2** can be done using ANSYS graphical user interface (GUI). Another important, ANSYS use SI unit for the calculation. Therefore the pressure in English unit, pound square inch (psi) must be converted to SI unit, Pascal (Pa). Conversion software can be used, as shown in **Figure 5.3**.
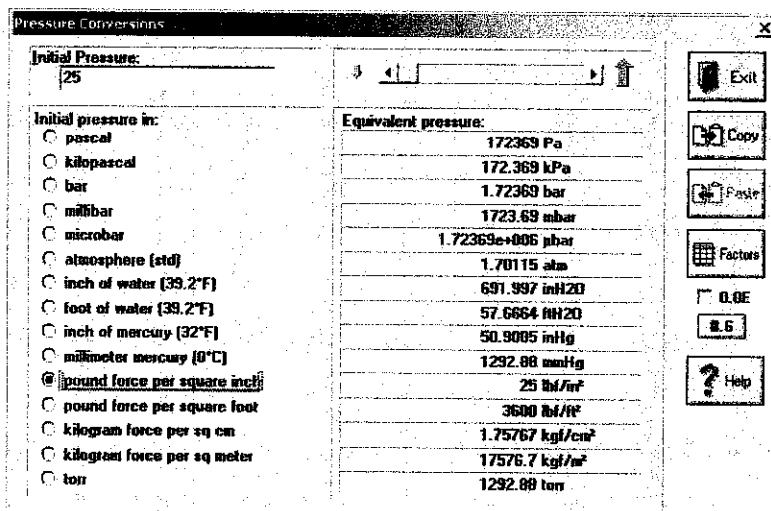
Figure 5.3: Conversion software for getting the pressure in Pascal.

5.3.2 Meshing

Using ANSYS, the user can self determine the style of mesh, as desired. In the simulation, some portion of the drawing needs to be meshed with high number of nodes in order to get a more detail and accurate result. The concentration of meshing was determined by the number of elements for each line of the drawing. The areas that need detail meshing are shown in **Figure 5.4**. The circled area is the area that has the most probability for the vena contracta to occur. The essential results to be analyzed are the vector plot of the velocity and the contour plot for pressure.
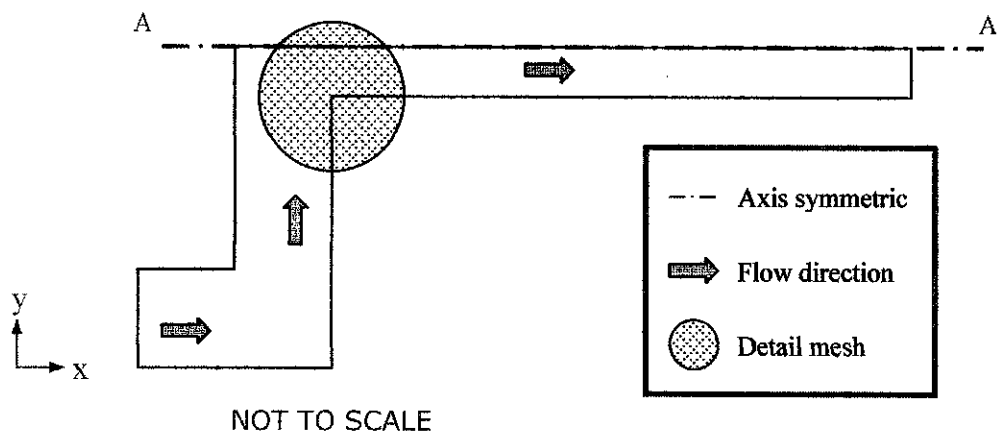
Figure 5.4: Area with high mesh concentration

5.3.3 Adequate meshing justification

The meshing must be justified to be adequate enough to get the accurate results and appropriate simulation time. Appropriate level of the meshing concentration must be set in order to get an adequate mesh. The coarsest mesh is the mesh with very little number of elements while the finest mesh has too much number of elements.

The single-phase simulation must be done according to the set of meshing (from finest to the coarsest) as shown in the **Figure 5.5** and **Tabl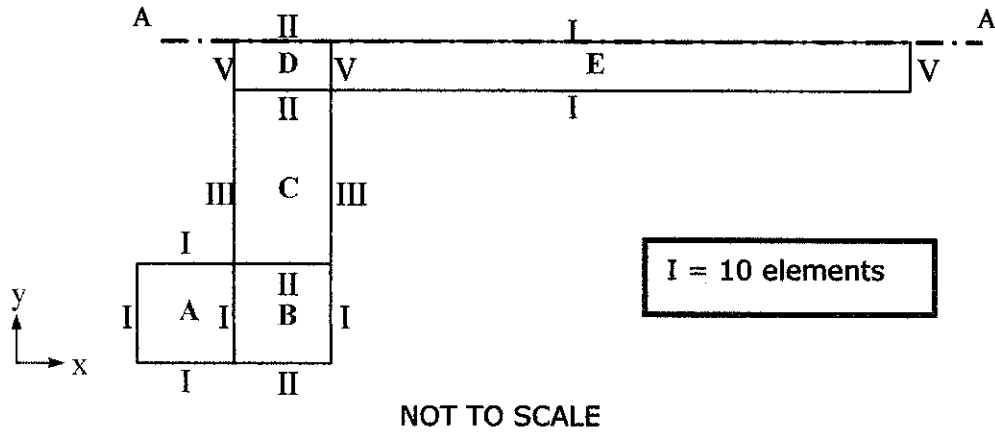e 5.1**. The comparison for velocity plot and nodal solution (pressure) were done for all set of results. The solution with the most accurate result and the most similar with finest result will be selected. The notation I, II, III, IV and V are referring to the mesh division for each line. While A, B, C, D and E will refer to the area of the specific location.

NOT TO SCALE

Figure 5.5: The mesh division in each line.

Set	II		III		IV		V	
	No. of elements	Spacing Ratio	No. of elements	Spacing Ratio	No. of elements	Spacing Ratio	No. of elements	Spacing Ratio
1	10	5	20	5	40	5	12	5
2	15	5	30	5	50	5	15	5
3	15	5	25	5	60	5	15	5
4	15	5	30	5	60	5	20	5
5	15	5	30	5	70	5	20	5
6	15	5	30	5	80	5	20	5
7	30	5	30	5	90	5	30	5
8	30	5	30	5	100	5	40	5
9	35	5	50	5	100	5	40	5
10	40	5	60	5	100	5	40	5
11	50	5	70	5	120	5	40	5

Table 5.1: Set of meshing with different number of elements

The number of elements refers to the quantity of elements in the certain rows and column in the meshing area. While the spacing ratio is the ratio of how many elements concentrate at certain part in the drawing. It means that, more number of elements will concentrate at one part of the drawing as specified by the user. As example, if spacing ratio is one, the element will be distributed equally. But if spacing ratio is more than one the concentration is bias at one side of specified location. **Figure 5.6** shows the illustration for the mesh result, which is set 6. The mesh justification will be done according to the accuracy of the results using an adequate meshing concentration. An accurate and easier calculation for simulation requires a mapped mesh (see **Figure 5.7**). Mapped mesh allowed the elements is arranged uniformly. Therefore, the calculation for the simulation can be done easily using array method (7).
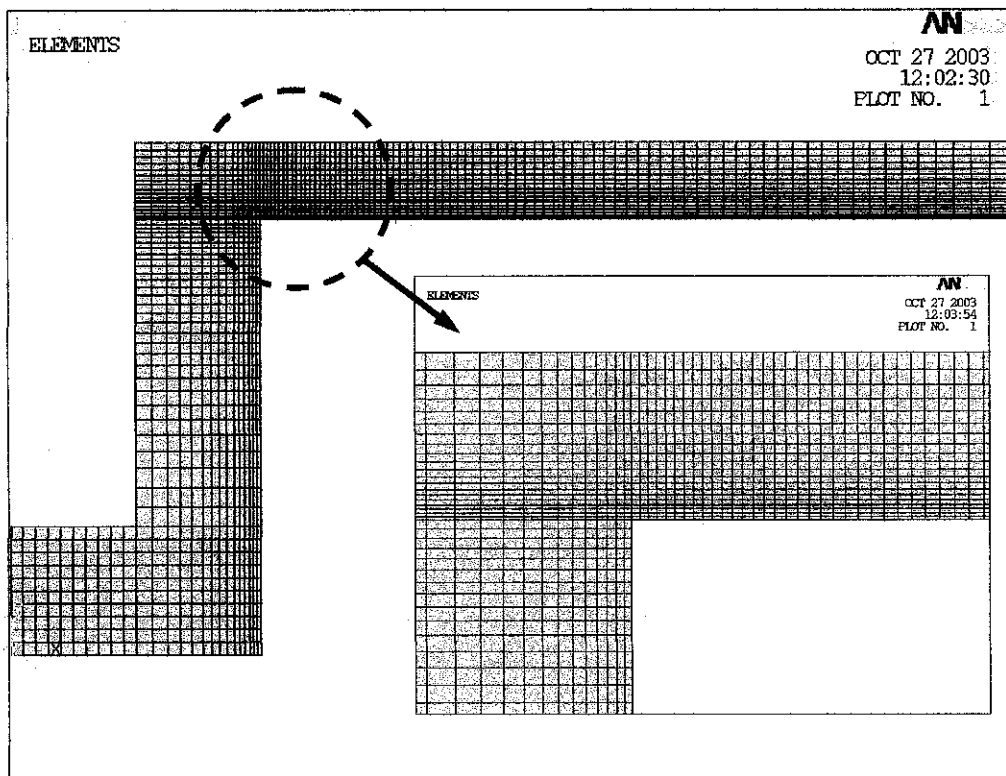
Figure 5.6: Mesh result (mapped) for set 6 from ANSYS GUI.
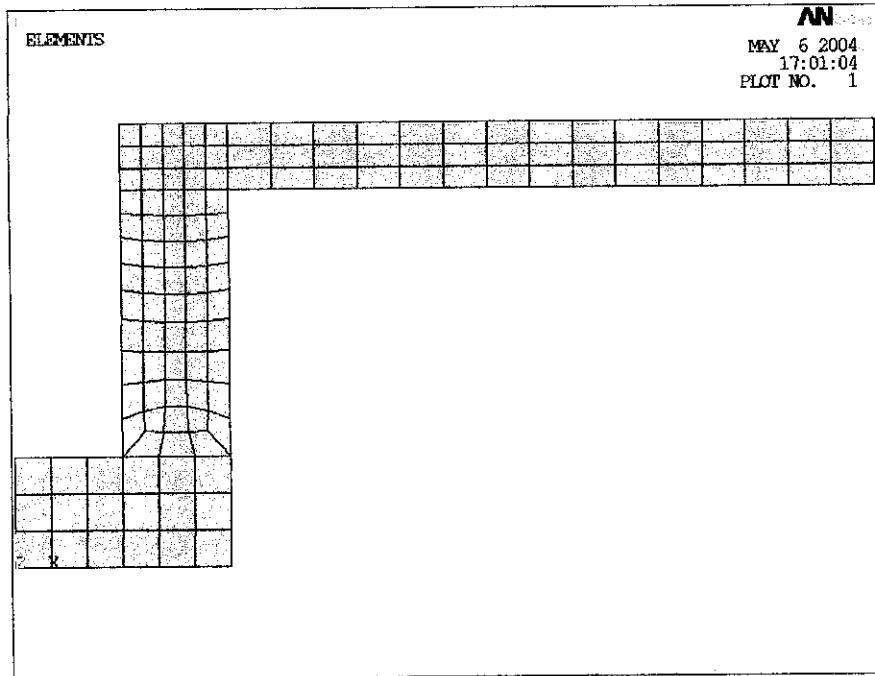
Figure 5.7: Mesh result (free mesh) from ANSYS GUI.

5.4   Volume of fraction (VOF) analysis

The VOF analysis is an additional procedure to the FLOTRAN simulation (7). All the parameters are set in the same manner provided with the steps as shown in the process flow diagram in **Figure 5.8**. The analysis is used to determine the volume fraction for the internal flow pattern in the nozzle. If there is a bubble, the volume fraction will be less than one. The cavitation will result changes in the volume of liquid-vapour fraction in the fluid flow. Therefore the simulation result is expected to show the contour plot of vapour fraction (VFRC). The sharp inlet nozzle area is focused because cavitation is suspected to occur there. The governing equations for the 2-phase model of VOF analysis are shown in **Appendix 5.1**.
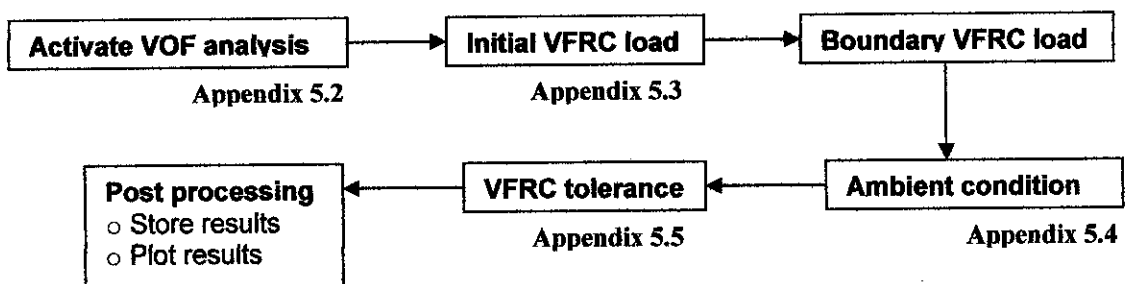
Figure 5.8: Process flow diagram of VOF analysis

5.5   Solving CFD Problem

The CFD problem could be solved by the convergence or divergence and stability of the analysis. It could be done by observing the rate of change of the solution and the behaviour of relevant dependent variables. These variables include velocity, pressure, temperature, and (if necessary) turbulence quantities such as kinetic energy (degree of freedom ENKE), kinetic energy dissipation rate (ENDS), and effective viscosity (EVIS). In this project the governing variable is pressure. The change in pressure will determine the flow behaviour in the nozzle.

As the FLOTRAN simulation proceeds, ANSYS calculates *convergence monitors* for each degree of freedom for global iteration. The convergence monitors are a normalized measure of the solution's rate of change from iteration to iteration (3). Denoting by the general field variable, ϕ, any DOF, the convergence monitor is defined as follows:

$$ConvMon = \frac{\sum_{i=1}^{N} \left| \phi_i^k - \phi_i^{k-1} \right|}{\sum_{i=1}^{N} \left| \phi_i^k \right|}$$

The convergence monitor represents the sum of changes of the variable calculated from the results between the current k_{th} iteration and the previous $(k-1)^{th}$ iteration, divided by the sum of the current values. The summation is performed over all n nodes, using the absolute values of the differences.

Figure 5.9 (a) and **(b)** will illustrate the convergence monitors displayed by the Graphical Solution Tracking (GST) feature for steady state and transient cases. However the figures only show the curve pattern for both cases, but not the exact GST for the project simulation.

Time = 0

Cumulative Iteration Number (a)

Time = 1.23435E+02

Cumulative Iteration Number (b)
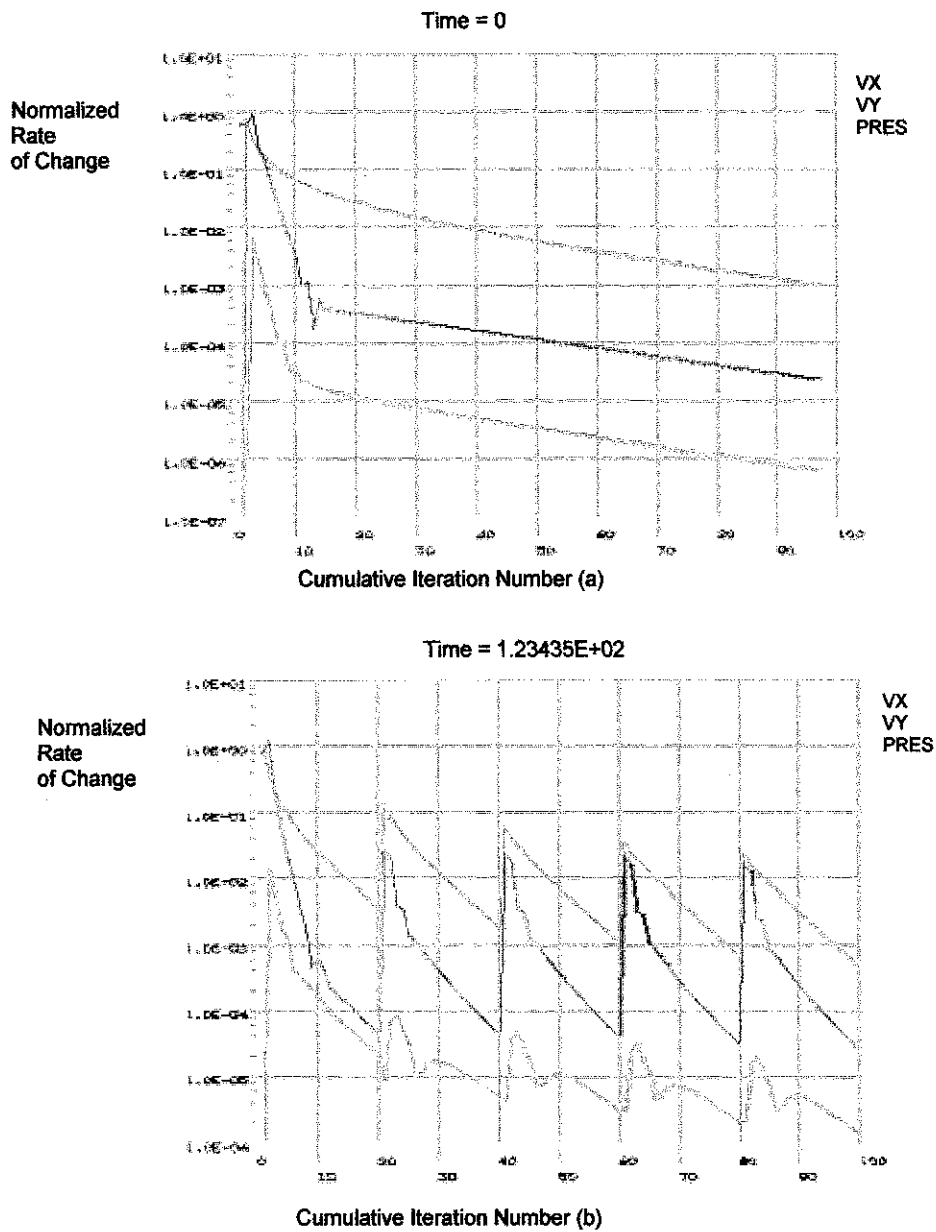
Figure 5.9: Convergence monitors displayed by the Graphical Solution Tracking (GST) feature. (a) Steady-state simulation (b) Transient simulation

Figure 5.9 (b) is a plot of a transient FLOTRAN solution. Each "spike" on the plot indicates the beginning of a new time step. Perhaps after some initial fluctuations, convergence monitors will decrease as the analysis approaches convergence. The convergence number depends on several factors, such as:

- Complexity of the geometry
- Adequacy of the finite element mesh in regions with steep gradients

27

- The severity of the turbulence levels, indicated by the flow Reynolds number
- How well developed the flow is near outlet boundaries.

5.6   Examining the Results

The users can post process output quantities and examine the results in the output files. This process required engineering judgment when examining the results to evaluate the plausibility and consistency of the overall analysis approach, how specific properties are used, and the conditions imposed.

CHAPTER 6

RESULTS & DISCUSSION

6.1 Introduction

This chapter consists of the results of the simulation for single phase and two phase flow. The results for the simulation are displayed in vector plot especially for velocity profile. For vector quantities, arrowheads are used since they illustrate a more accurate picture of the actual flow profile. On the other hand, the variables like pressure and volume fraction (2-phase analysis) are displayed by the colour-filled contour map.

Basically the single phase flow is used to determine the appropriate mesh concentration for the simulation model, which will be applied through out the project. Moreover, the internal flow characteristic also can be determined from the result. The interpretation of the flow pattern was done by comparing the simulation output with the experimental results. Both results were explained by the theory on the internal flow phenomena of the diesel fuel injector. Therefore, the conclusion can be made to verify and explain the fluid flow behaviour in the injector with aid of simulation diagram.

The experimental results shows the hydraulic flip and cavitation flow occur because of the change in the operating pressure (see **Figure 4.5**). The CFD software must be able to model 2-phase flow at the same time. However, there were several limitations in ANSYS due to that matter, which will be discussed further at later section in this chapter. The 2-phase flow still can be modelled in ANSYS, but some extra steps need to consider while setting up the simulation model.

6.2　Selection of turbulence model

As mention in chapter 2, FLOTRAN offers six turbulence models. Several simulations at the same inlet pressure (25 psi) were modelled to compare the effect of changing the turbulence model mode for the simulation. The results were summarized in the **Table 6.1** below. The relevant result plots are for the pressure and turbulent K.E.

Turbulence Models (TM)	No. of Iteration	Minimum pressure (Pa)
1. Standard k-epsilon Model	999	-10874
2. Zero Equation Turbulence Model (ZeroEq)	710	-15915
3. Re-Normalized Group Turbulence Model (RNG)	910	-19444
4. k-epsilon Model due to Shih (NKE)	975	-19231
5. Non-linear Model of Girimaji (GIR)	10	0
6. Shih, Zhu, Lumley Model (SZL)	10	0

Table 6.1: Results due to change of turbulence model

The selection of turbulence model was based on the output of the internal flow simulation (see **Appendix 6.1**) and the table above. The minimum pressure occur at cavitation point (for TM 1-4) is different. The minimum pressure range was big for some of the model. For turbulence model 5 and 6, the results from the simulation shows very different pattern for nodal solution. The plot is too simple and the result may not be acceptable for analysis.

The results show that turbulence model 1 until 4 give a quit similar pressure plot. But base on the turbulence model theory, the third TM, Re-Normalized Group Turbulence Model (RNG) was selected for the modelling project. RNG is effective where the geometry has a strong curvature (e.g., a duct that goes through a 180 degree change in direction). In this project, the sudden changing of flow direction occur and has a curvature angle is about 90 degree. Therefore RNG Turbulence model will be the appropriate model to choose. For this project the TM 1 and TM 2 still can be used since the analyzed shape is simple. However, for TM 4, the models are recommended for rotating flow.

6.3   Single phase flow – sharp inlet nozzle

Table 6.2 shows the results obtained from the simulation using a different set of meshing concentration as shown in the previous chapter (refer **Table 5.1**). The lower mesh concentration, the shortest simulation time will be. The adequate meshing for this simulation had already justified in the previous chapter. The mesh concentration value is between the coarsest and the finest mesh. Therefore, the simulation time will be reduced using an adequate meshing instead of using the finest mesh. The good result still can be obtained using the adequate mesh. Hence the computational cost can be reduced

Set	Simulation Time (min)	No. of Iteration
1	18	750
2	19	755
3	14	999
4	30	1050
5	70	1720
6	80	1830
7	170	2315
8	190	2520
9	240	5460
10	240	5460
11	300	7200

**Table 6.2**: Simulation results for 25 psi inlet pressure

In order to find the adequate meshing, the simulations were done with the finer and coarser meshing as shown in the initial setup in set 1. From the results it shows the sudden pressure drop occur at the area after the separated flow. For this result, the cavitation did not occur since the analysis in single phase flow. Cavitation only occurs at 2-phase flow. **Figure 6.1 (a)** and **(b)** at next page show the example for velocity plot and the pressure plot taken from set 6. All the results obtained, have quite similar pattern of fluid flow. Only one set of the above will be selected for the most adequate meshing on getting a good result.

Cavitation effect in the fluid flow occurs due to sudden change of direction such as junction or any restriction in the flow profile. It results in a pressure drop at the area. The higher pressure different will cause the changing in flow from cavitation to hydraulic flip.

31

Interpretation from that concept, the cavitation effect at 25 psi occurs only at the second junction (inlet nozzle). At that junction, a small portion of the contour plot has a severe pressure drop. The cavitation effect seems to be insignificant due to most probably single-phase (liquid) flow was set during simulation. Theoretically, greater effect of cavitation will be observed in the 2-phase (liquid and gas) simulation flow.
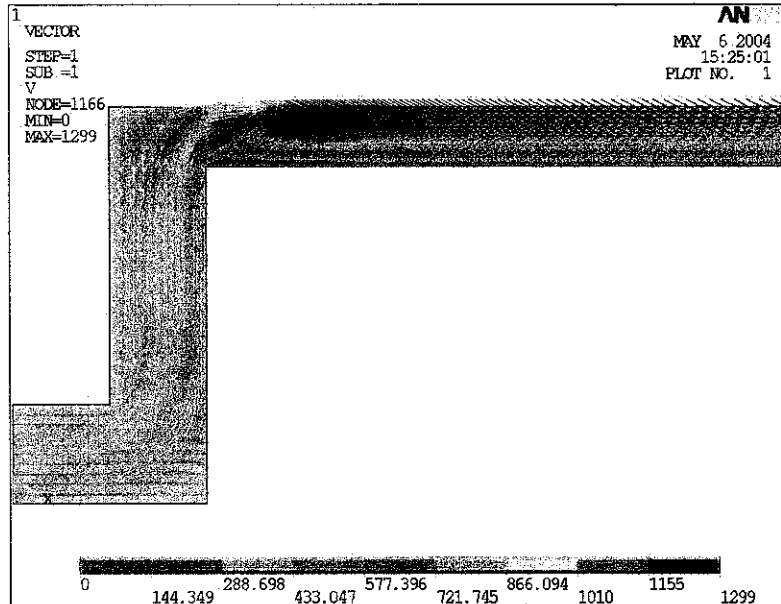
(a)
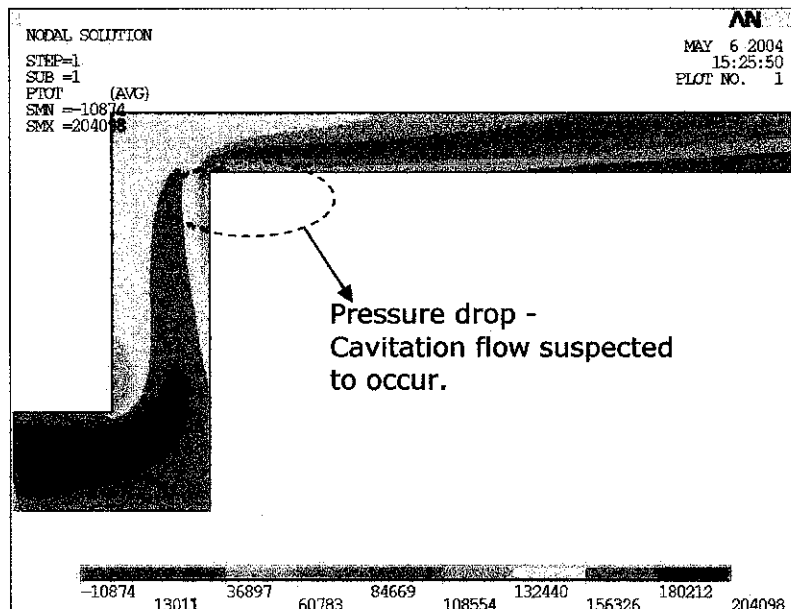
(b)

Figure 6.1: Results for set 6, (a) Velocity – vector plot (b) Pressure – contour plot
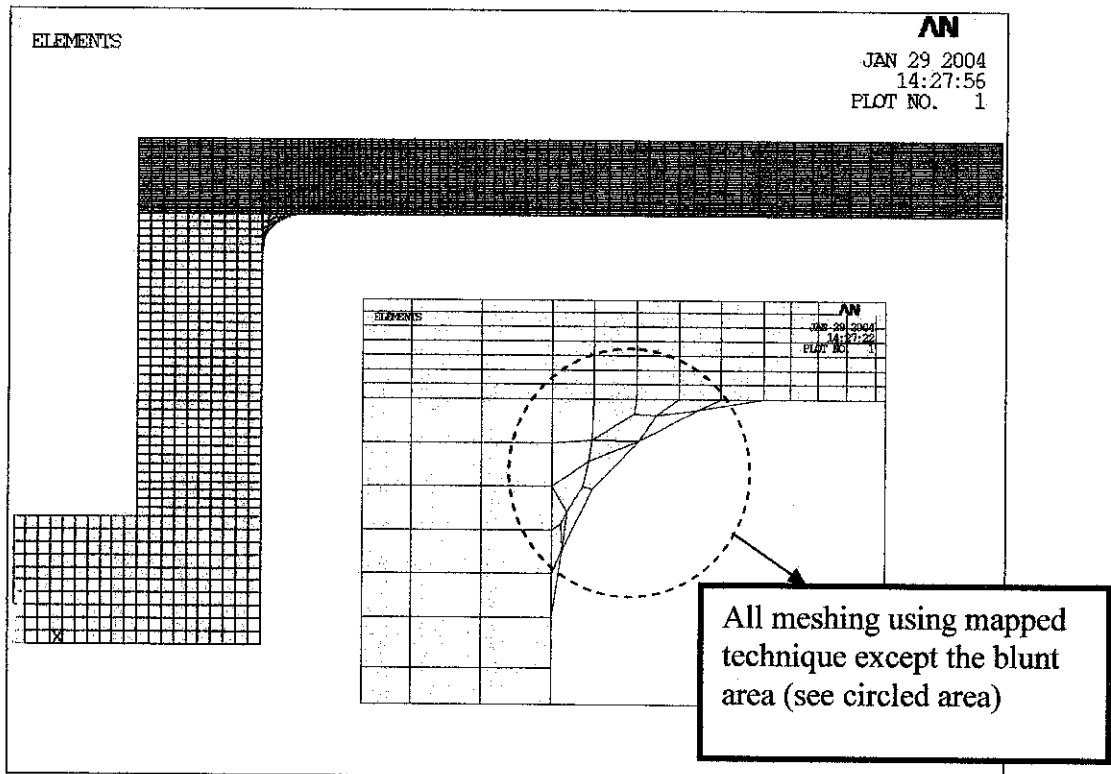
After comparing the results, it was found that the flow pattern at the circled area (refer **Figure 6.1 (b)**) shows the vena contracta behaviour. Normally, when cavitation occurs, the flow is disturbed by this effect and lead to generation of atomisation flow at the outlet nozzle. The atomisation occurs because of the cavitation in the internal flow. The atomisation flow will be needed for the combustion process in order to ensure a complete combustion and reduce the emission. For this project, an accurate result will be determined by the relevancy with experiment data. However some of the results from the set of meshing did not really show exactly like the results for finest set. This is suspected due to several factors:

- Not enough meshing concentration
- No continuation meshing from the inlet to the outlet area of the injector. (in term of number of element)
- The detail meshing not concentrate at the circled area (**Figure 5.4**)
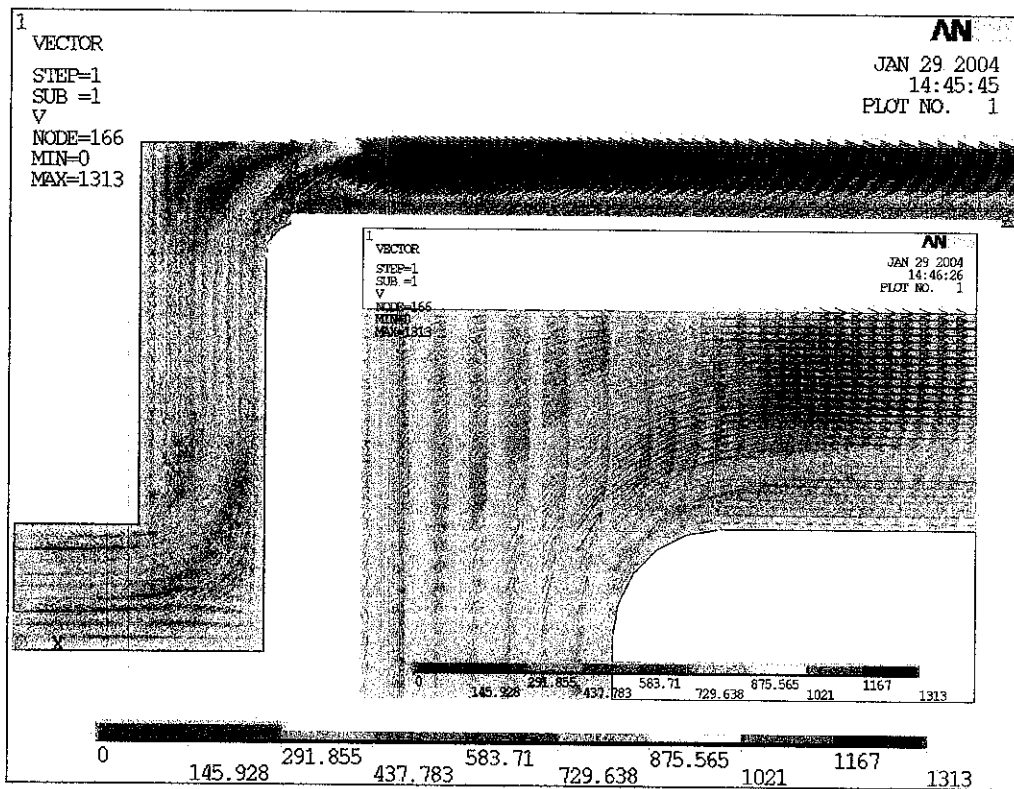
For set 6, the meshing concentrated at the circled area like shown at **Figure 5.7** in the previous chapter. The result of pressure plot and velocity plot for this set was compared with the finest meshing which is set 11. It showed the similarity between these two results. It means that the simulation outcome from set 6 is adequate enough to model the internal flow behaviour and get the accurate result. Therefore set 6 is selected as the meshing concentration module for this simulation. Moreover, the simulation period for this set is smaller compare with other accurate result.

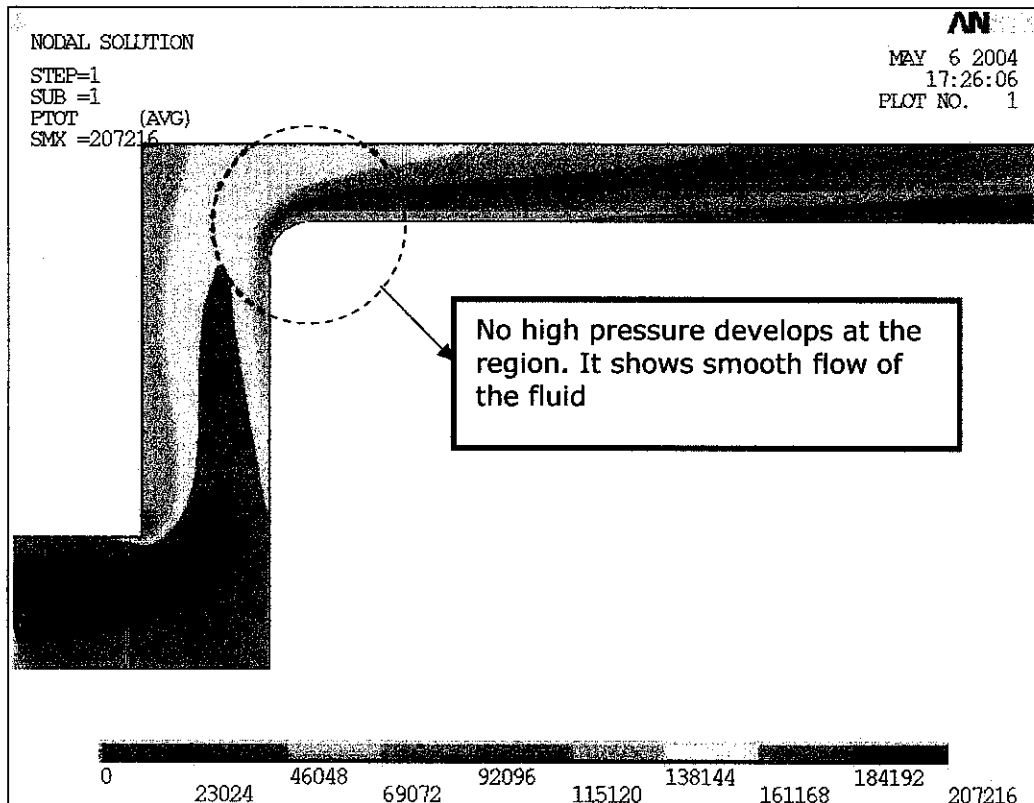## 6.4   Single phase flow – blunt inlet nozzle

The simulation was done in 2-dimensions by using the axis-symmetric theorem similar to the sharp inlet nozzle. The actual injector that is used is normally blunt due to the machining process of making the injector. The meshing concentration for this model follows the selected meshing set in the sharp inlet nozzle part except for the blunt area. It will be better if the mesh can be done using 'mapped mesh'; therefore accurate calculation will be achieved. **Figure 6.2** shows the mesh result for the blunt inlet nozzle model. The simulation proceeds with this meshing and the results obtained as **Figure 6.3** and **Figure 6.4.**

33

ELEMENTS

JAN 29 2004
14:27:56
PLOT NO.   1

All meshing using mapped
technique except the blunt
area (see circled area)

Figure 6.2: Mesh result (mapped) for blunt inlet nozzle except the blunt area.

VECTOR

STEP=1
SUB =1
V
NODE=166
MIN=0
MAX=1313

JAN 29 2004
14:45:45
PLOT NO.   1

0   291.855   583.71   875.565   1167
   145.928   437.783   729.638   1021   1313

Figure 6.3: Velocity plot for blunt inlet nozzle at 25 psi.

Figure 6.4: Pressure plot for blunt inlet nozzle at 25 psi.

The results above have slight difference with the previous sharp inlet nozzle at the blunt area (see circled part at **Figure 6.4**). There is no high pressure at the area, which means that less or no cavitation effect occur. If compared with the sharp inlet nozzle, the will be smoother and less atomisation will produced.
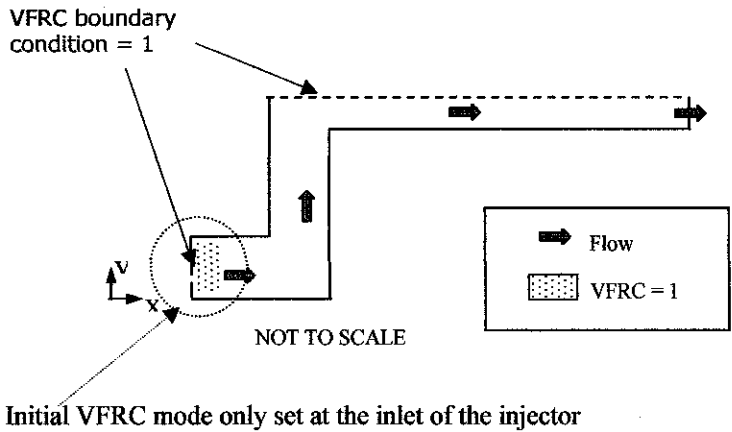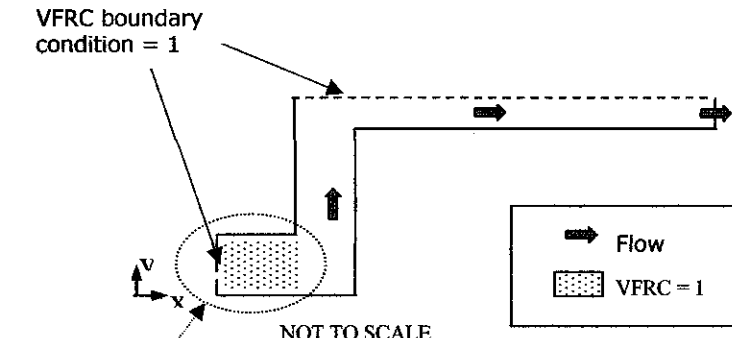
## 6.5 2-phase flow using volume of fluid (VOF) analysis

The aim for this VOF analysis is to get the plot for volume fraction of the fluid flow in the nozzle. As mentioned in the previous section, the interested area to focus is at the inlet of the nozzle (circled area, see **Figure 6.4**). From the volume fraction pattern (VFRC plot), the behaviour of fluid flow at the nozzle outlet can be predicted. Cavitating flow at the nozzle outlet is due to the cavitation that occurs at the nozzle inlet. This cavitating flow will produce a break-up of fluid flow into smaller droplets which increase surface area of the fluid. Therefore the plot at the nozzle inlet area must have volume fraction less than 1. However, if less or no cavitation occurs at the nozzle inlet the

outflow pattern should be a hydraulic flip (condition where flows straight out from the nozzle), while the volume fraction will be almost 1 at all area in the nozzle.

6.5.1 VFRC setting with inlet pressure at 25 psi

Before proceeding with the detailed modelling, the project is continued with several simulations which focused on finding the appropriate setting for initial VFRC option in ANSYS. The appropriate setting will be chosen using the 3 different setting in **Table 6.2**. The results were compared between inlet pressure of 25 psi (severe cavitation) and 190 psi (hydraulic flip). The setting will be based on the understanding of the ANSYS manual and on trial and error basis. The set of simulations are as follow.

Set No.	Sketch of initial volume fraction (VFRC) setting and description
1	VFRC boundary condition = 1 NOT TO SCALE Flow VFRC = 1 Initial VFRC mode only set at the inlet of the injector
2	VFRC boundary condition = 1 NOT TO SCALE Flow VFRC = 1 Initial VFRC mode was set at the inlet area of the injector as shown in the picture.

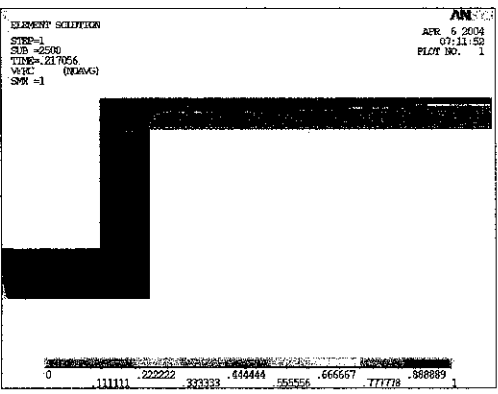| 3 |

Initial VFRC mode was set at the inlet area until just before the nozzle inlet of the injector as shown in the picture. |
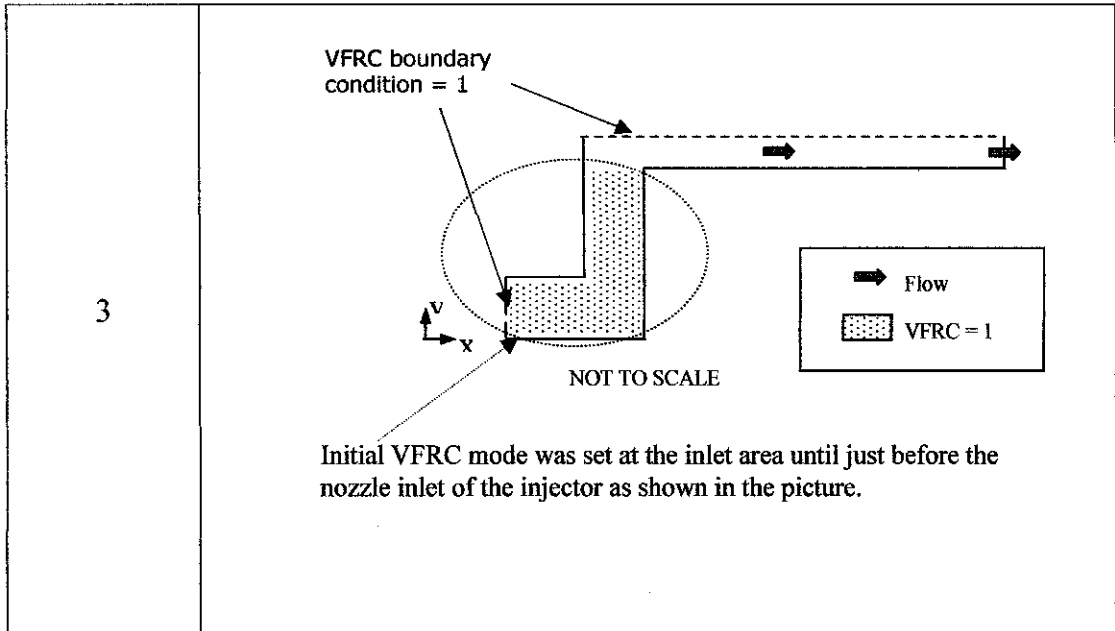
Table 6.3: 3 different set for initial VFRC setting
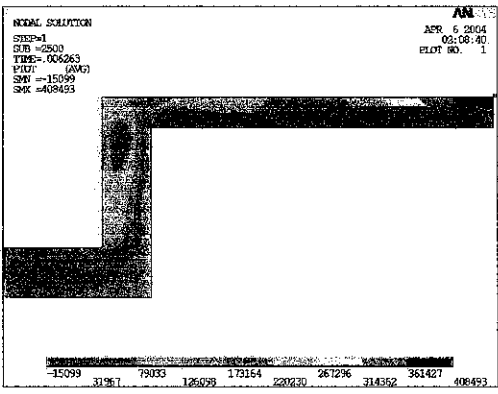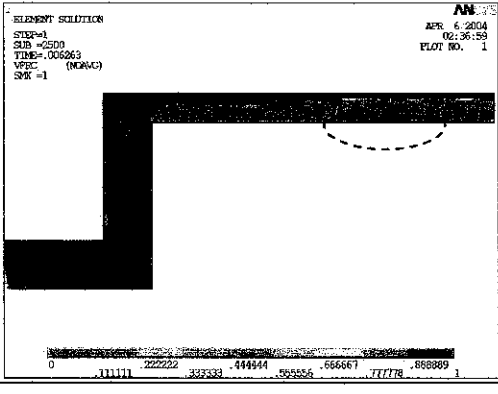
The results are summarized in **Table 6.4, Table 6.5** and **Table 6.6** at next page.

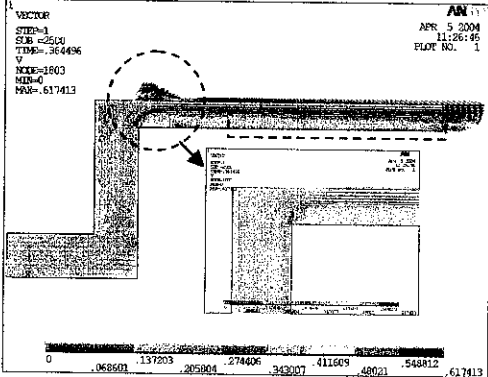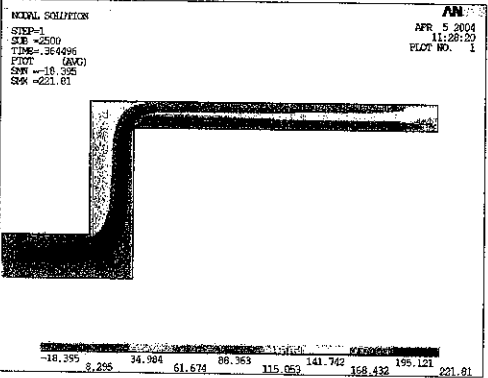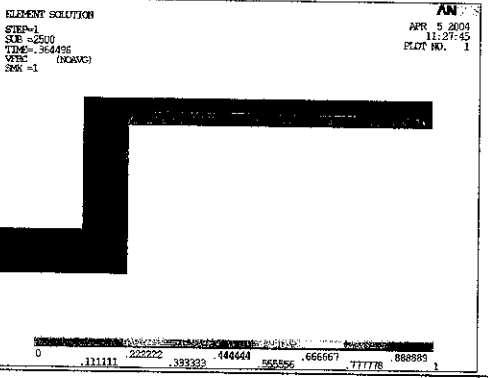| Set No.	Simulation result	Remarks
1	Pressure plot: 	o The blue region is the lowest pressure part. It occur after the fluid entering the nozzle and up until at the outlet. o This set of simulation didn't show a back flow region. It maybe because of the small value of fluid element is set.

VFRC plot:		o Red area is when VFRC equal to 1, while blue area is when VFRC is almost zero.
		o At the lowest pressure, the VFRC is almost 0.
		o It means that, the flow is in the 2-phase mode at some portion, after entering the nozzle area until the outlet of the injector.

Table 6.4: Results for set 1 of VFRC setting with inlet pressure setting at 25 psi

Set No.	Simulation result	Remarks
2	Pressure plot: 	o Similar with the previous set, the lowest pressure occurs at the section after the fluid enters the nozzle until at the outlet of injector. o High pressure drop after the fluid enters the nozzle.
	VFRC plot: 	o The 2-phase flow occurs at the lowest pressure area. o Some portion of fluid (circled area) shows the scattered flow at the nozzle area.

Table 6.5: Results for set 2 of VFRC setting with inlet pressure setting at 25 psi

38

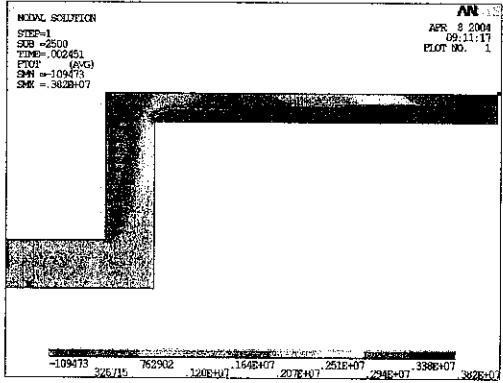| Set No.	Simulation result	Remarks
3	**Velocity plot:** **Pressure plot:** **VFRC plot:** 	o The circle part in the results is just an error in the display. o The exact flow pattern for that part is shown at the zoom in figure. o The rectangle area experience some back flow. o Low pressure occurs at the back flow area. o Low pressure and back flow indicate the cavitation case. o The outlet flow from this simulation results will experience atomisation flow due to cavitation phenomena after fluid entering the inlet nozzle. o The 2-phase condition occurs at the cavitation area. o Some fluid (red) can be observed at wall in the back flow area.

Table 6.6: Results for set 3 of VFRC setting with inlet pressure setting at 25 psi
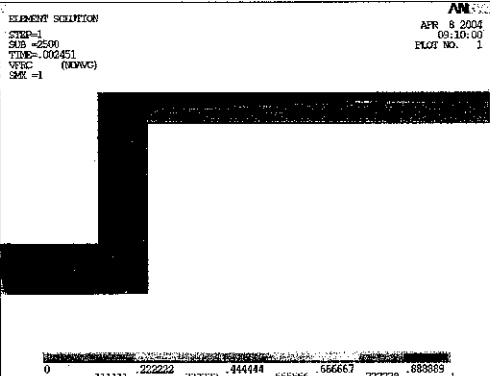
Simulation setting for set 1 and 2 were theoretically correct. Before any changes in direction or other external force to disturb the flow, the volume fraction of the fluid must be 100% or equal to one. Meanwhile for set 3, the simulation had already neglected the effect of changing direction in fluid to the flow behaviour. If small turbulence portion occur after the first fluid junction, the simulation might probably shown that the volume fraction will be less than one. In other word, if the VFRC is not 100%, the flow is supposed to have air or bubbles.

The results show the different flow behaviour for each set. Theoretically, according to the manual, the results for set 1 and 2 will be almost similar. But in all three sets, the volume fraction at the inlet area until just before the nozzle inlet area, it happens to be equal to one. It means that, the flow will be expected to be in single phase condition before the nozzle inlet area. Therefore the assumption made in simulation for set 3 is correct.
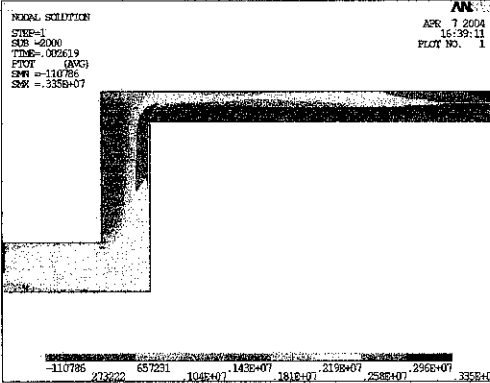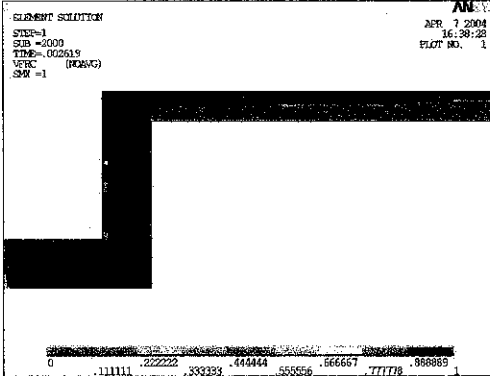
6.5.2 VFRC setting with inlet pressure at 290 psi

The project then focus on the simulation of the injector flow at 290 psi according to the three different set off initial VFRC setting. The set of setting can be referred at the previous section. The results was summarize in **Table 6.7, Table 6.8** and **Table 6.9**.

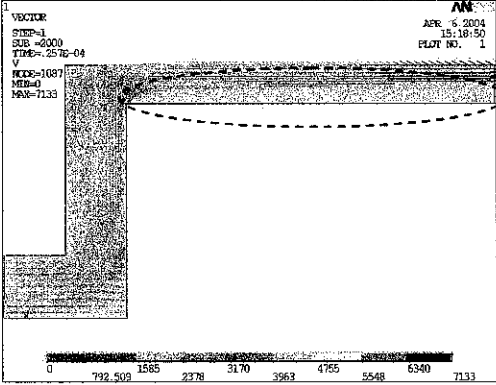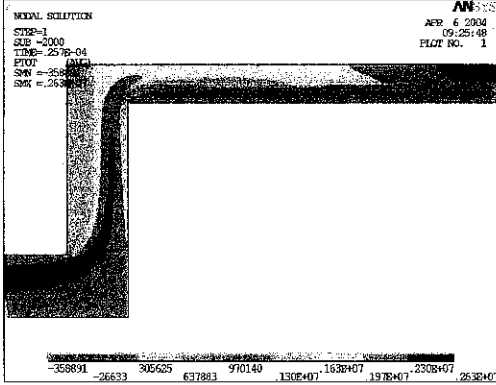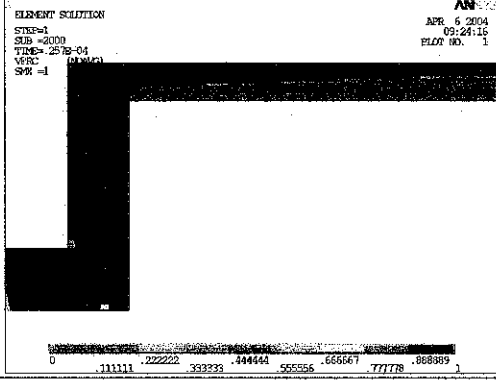| Set No.	Simulation result	Remarks
1	Pressure plot: 	o The blue region has the lowest pressure part. It occur after the fluid enter the nozzle and until reaches the outlet. o High pressure occurs at the end of the injector outlet.

	VFRC plot: 	o Red region is when VFRC equal to 1, while blue region is when VFRC is almost zero. o At the lowest pressure, the VFRC is 0. o The flow is in the 2-phase mode after entering the nozzle area until the outlet of the injector.

Table 6.7: Results for set 1 of VFRC with inlet pressure at 290 psi

Set No.	Simulation result	Remarks
2	Pressure plot: VFRC plot: 	o Similar with the previous set, the lowest pressure occurs at the section after the fluid enters the nozzle until it reaches the outlet of the injector. o The high pressure occurs at the outlet area of the injector. o The 2-phase flow occurs at the lowest pressure area.

Table 6.8: Results for set 2 of VFRC setting at 290 psi

Set No.	Simulation result	Remarks
2	**Velocity plot:** **Pressure plot:** **VFRC plot:** 	o The circled part in the results shows no back flow experience at the area after nozzle inlet. o The straight flow leaves the injector. o Very Low pressure only occurs at the junction of inlet nozzle. o The lighter blue indicates no fluid at that area which is clearly showed in the VFRC plot. o The 2-phase condition occurs at the area after inlet nozzle. o This is because of little or none fluid in contact at that area.

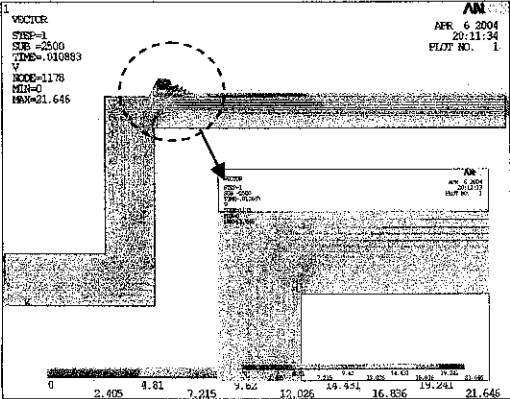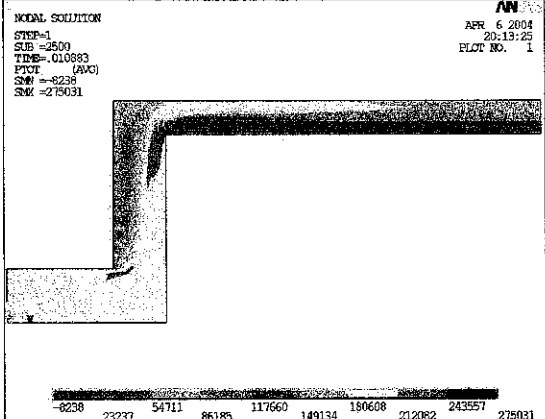**Table 6.9**: Results for set 3 of VFRC setting at 290 psi

42
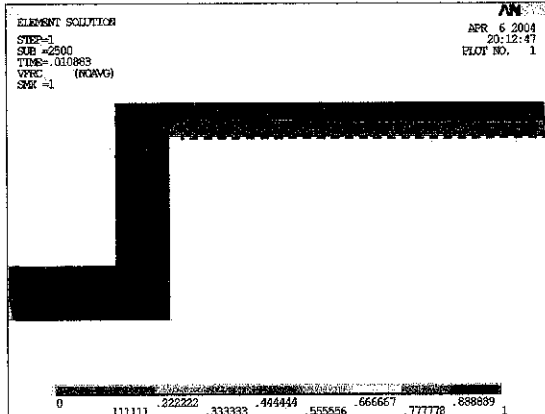
6.5.3 VFRC setting justification

From all the simulation results, the volume fraction at the injector inlet area until the nozzle inlet area is equal or almost to one. Comparing both 25 psi and 290 psi inlet pressure, it is appropriate to assume that the area mentioned is have initial volume fraction of one. Also in all cases, the flow after the inlet nozzle has almost the same behaviour, which is in the 2-phase flow. Only in set three, the cavitation phenomena can clearly be seen. This effect maybe due to the higher elements of initial value of VFRC stated for the simulation. However, the volume fraction stated is not constant throughout the simulation. It only shows how much element in the simulation region at early stage right at the beginning time and has no serious affect on the simulation results.

The limitation in the ANSYS is that; it is unable to plot the exact behaviour for the volume fraction plot results. VOF analysis can simulate 2-phase condition, but the result can only determine whether the flow in totally liquid or totally gas phase at certain area. The transition parts between the 2-phases are not clearly shown. This limitation was explained in the *ANSYS theory reference* (3). Based on the discussion the third set will be chosen as a comparison due to the nearest similarity with the experimental results.

6.5.4 VFRC setting with inlet pressure at 26 psi

VOF analysis continued with the interchange pressure where the flow was changing from severe cavitation to the hydraulic flip flow. It is important to observe how the internal fluid flow reacts to the crucial pressure at 25 psi and 26 psi. The results were summarised in **Table 6.10.**

43

Simulation result	Remarks
Velocity plot: 	o The circled part is just error in the display. The exact flow pattern is like the zoom in figure o The straight flow leaving from the injector. o At zoom in picture, no back flow occurred.
Pressure plot: 	o Low pressure occurs only at the junction of inlet nozzle until the injector outlet.
VFRC plot: 	o The 2-phase condition occurs at the area after inlet nozzle. o The flow after inlet nozzle until the injector outlet, little or none fluid in contact at the rectangle area.

Table 6.10: Results for VFRC setting with inlet pressure at 26 psi

6.6   Software restriction and limitation

This simulation project deals with ANSYS software only. Similar with other software, there are always some limitations that avoid user from getting highly accurate results. In the following reports are brief discussion on the limitation and restriction for this software (4).

6.6.1   ANSYS / FLOTRAN limitation

o   The simulation must be done using the transient mode which requires a longer execution time compared to the steady state analysis.

o   For the initial VFRC field, each element is defined as initially full, partially full or empty. Each partial element must be adjacent to at least one full element and one empty element. During the analysis, if a partial element does not have any full elements as neighbours, it will be reset to empty. At least one layer of empty elements must be included above the free surface to allow the surface to evolve in time. Therefore initial value must be set in order the VOF analysis to execute.

o   By default, the volume fraction is zero. Therefore, if there is fluid initially inside the problem domain, the user must set the VFRC field accordingly. Unfortunately, with different value of initial VFRC setting, the slightly different results obtained at the nozzle area.

o   In the FLOTRAN solution routines, a nearly empty element adjacent to a nearly full element may introduce a sudden change in the locally rescaled meshes. This can make the stiffness matrix more ill-conditioned and can adversely affect the quality of the desired solution.

o   For a VOF analysis, the density is constant. Therefore, mass conservation is equivalent to the conservation of the total fluid volume (or area in two dimensions). Ideally, the difference between the volume coming into the problem domain and going out of the domain should be equal to the increase or decrease of the total volume inside the domain. In an actual finite element analysis, however, continuity satisfaction is expressed in a Galerkin weak form. Therefore, in general, each element has a small mass imbalance. The local mass imbalance is usually of the

order of the discretization error, and this error is a major source of the global VFRC imbalance introduced in a VOF analysis. Even though this imbalance may be very small compared to the total volume, it can accumulate exponentially as the number of time steps increases.

o The VOF advection time step is set equal to the solution time step divided by a factor that the user specifies. If the VOF advection time step is still too large, FLOTRAN will automatically reduce the VOF time step by half. This automatic reduction in the VOF time step continues until the local imbalance of the VFRC field during the VOF advection computations is less than the VOFL tolerance. A good input parameter guess makes the calculation more efficient by removing some checks on the time step. It means that, the user have to specify a good guess advection time for getting a good results.

6.6.2   Assumptions and Restriction for FLUID141

The element must not have a negative or a zero area. The connectivity of an element with the nodes must be defined in counter clockwise order. The element must lie in the X-Y plane. The following assumptions have been made in the formulation:

- The nodal coordinate system and the global coordinate system must remain the same.
- The problem domain and the finite element mesh may not change during an analysis.
- The fluid is a *single phase fluid*; results for 2-phase flow will be restricted with some error.
- Free surfaces are not permitted.
- In the incompressible option, work done on the fluid by pressure forces, viscous dissipation, and kinetic energy terms are neglected in the energy equation. The incompressible energy equation is a thermal transport equation

CHAPTER 7

CONCLUSION AND RECOMMENDATION

7.1   Relevancy to the objectives

o   The computational cost will be reduced if the simulation is done using an adequate set of meshing and the accurate result can be obtained.

o   The flow pattern for the sharp inlet nozzle and blunt inlet nozzle can be studied using a pressure contour plot and velocity vector plot.

o   The internal flow characteristic (atomisation and hydraulic flip effect) can be observed in the simulation results.

o   ANSYS software is able to model the 2-phase flow cases with some limitation which require user interpretation and appropriate setting.

7.2   Suggested future work for expansion and continuation

o   To model the 2-phase simulation for blunt inlet nozzle for comparison with the sharp inlet nozzle. In this project, the 2-phase analysis only focuses on sharp inlet nozzle. Therefore, it will be very useful to know the internal flow behaviour for blunt inlet nozzle.

o   To determine the effect of flow pattern by varying the inlet nozzle shape. (ie. Blunt inlet or diagonal shape with certain angle). The information from this simulation can be used for designing a diesel injector. The experimental results can be referred to the Y.Laoonual et. al. (6) research paper for verification.

o   To do the same simulation process with different CFD software or later version of ANSYS since the results obtain from this project are due to the several limitation and restriction. Hence, the results from this simulation can be compared with others.

REFERENCES

1. Willard W. Pulkrabek, *Internal Combustion Engine*, Prentice hall International, Inc, USA, 1997

2. Saeed Moaveni, *Finite Element Analysis – Theory and Application with Ansys*, PRENTICE HALL, Upper Saddle River, New Jersey. 1999

3. *ANSYS Theory References*, http://sun1.rrzn-user.uni-hannover.de/jgaertner/ansys61/JavaHelp/content/theory_toc.html

4. *Final Year Project Guidelines for Supervisors and Students*, Semester July 2003, Universiti Teknologi PETRONAS.

5. A M Dalli, *"Transient Cavitation and Separation in Scaled-up Model of a VCO Orifice"*, Department of Mechanical Engineering, UMIST, Manchester, England, *14th ILASS-Europe 1998*, Oxford Laser Ltd.

6. Y.Laoonual, A.J.Yule and S.J.Walmsley, (Atomisation and Sprays Research Group) *"Internal Fluid Flow and Spray Visualization for a Large Scale Valve Covered Orifice (Vco) Injector Nozzle"*, Department of Mechanical Engineering, UMIST, Manchester, England

7. *ANSYS 6.0 User manual*, http://sun1.rrzn-user.uni-hannover.de/jgaertner/ansys61/JavaHelp/content/manual_toc.html

8. R I K Shazi, 1999, *"Simulation of Internal Fluid Flow in a Diesel Injector Using Commercial CFD Code Fluent"* Final Year Project Report, University of Manchester Institute of Science and Technology (UMIST).

9. Donald F. Young, Bruce R. Munson, 2001, *A Brief Introduction to Fluid Mechanics*, second edition, John Willey & Sons, INC. New York

17. *Diesel injector principle*, http://www.howstuffwork.com

APPENDIX 2.1: 6 Turbulence Model in ANSYS software

1. Standard k-epsilon Model (default)

The Standard k-epsilon Model and the Zero Equation Turbulence Model are the simplest models. The other four models are all extensions of the Standard k-epsilon Model. The Standard k-epsilon Model is the default model.

Cm, C1, C2, SCTK, and SCTD are Standard k-epsilon Model constants that are defined as follows:

Cμ - *Value* is the k-epsilon turbulence model constant

$$\mu_t = C_\mu \frac{\rho k^2}{\varepsilon}$$

which is used in the update of the turbulent viscosity.

C1 - *Value* is the k-epsilon turbulence model C1 constant. It is the multiplier of the shear rate generation term of the turbulent kinetic energy dissipation rate equation.

C2 - *Value* is the k-epsilon turbulence model C2 constant. It is the multiplier of the dissipation source term in the turbulent kinetic energy dissipation rate equation.

SCTK - *Value* is the Schmidt number for the turbulent kinetic energy. The diffusion term in the turbulent kinetic energy equation is divided by this factor.

SCTD - *Value* is the Schmidt number for the kinetic energy dissipation rate. The diffusion term in the dissipation rate equation is divided by this factor.

The following five wall parameters control turbulence wall modeling. The wall parameters apply for all turbulence models except the Zero Equation Turbulence Model.

KAPP - *Value* is the law of the wall constant. It is the slope of the plot of normalized shear velocity (u^+) versus the non-dimensionalized distance from the wall (y^+). See *ANSYS Theory Reference* for details.

EWLL - *Value* is the law of the wall constant. It is related to the y intercept value for a plot of normalized shear velocity (u^+) versus the non-dimensionalized distance from the wall (y^+). See the *ANSYS Theory Reference* for more details.

WALL - *Value* is the choice of wall conductivity model. The default model is the Van Driest model (*Value* = VAND), used most often for high Prandtl number fluids. The second choice is the Spalding model (*Value* = SPAL), applicable to low Prandtl number fluids. The third choice is the Equilibrium model (*Value* = EQLB). The equilibrium model is also automatically invoked for the wall viscosity by this command.

VAND - *Value* is the constant in the Van Driest wall conductivity model. See the *ANSYS Theory Reference* for details.

TRAN - *Value* is the magnitude of y^+ marking the outer boundary of the laminar sublayer. Used only for the Equilibrium Wall model.

The following three buoyancy terms control buoyancy modeling. The buoyancy terms apply for all turbulence models except the Zero Equation Turbulence Model.

BUC3 - *Value* is the k-epsilon buoyancy model constant. A value of zero means that there is no contribution to the turbulent kinetic energy dissipation rate equation. A value of zero is appropriate for stably thermally stratified flows.

BUC4 - *Value* is the k-epsilon multiplier applied to the buoyancy term of the turbulent kinetic energy equation. A value of 1.0 is appropriate for the calculation of stably thermally stratified flows.

BETA - *Value* is ß, the coefficient of thermal expansion

53

$$\beta = \frac{1}{\rho} \frac{\partial \rho}{\partial T}$$

This term is used in the buoyancy terms of the k-epsilon model.

2. Zero Equation Turbulence Model (ZeroEq)

The Zero Equation Turbulence Model (ZeroEq) is the simplest and fastest turbulence model. It applies to problems with fairly simple geometry and flow characteristics. The model does not give accurate results if there is significant separation or recirculation.

The Zero Equation Turbulence Model contains an automatic calculation of the length scale or you can specify the length scale. Generally, the turbulence ratio can be set to 2.0 when you are using the Zero Equation Turbulence Model.

3. Re-Normalized Group Turbulence Model (RNG)

The Re-Normalized Group Turbulence Model (RNG) is effective where the geometry has a strong curvature (e.g., a duct that goes through a 180 degree change in direction. If you have tried the SZL Model and the results are unsatisfactory, it is generally recommended that you try the RNG Model.

The RNG Model is an extension of the Standard k-epsilon Model. Seven constants are assigned values. The Cm, C1, C2, SCTK, and SCTD constants are assigned values that are separate from the Standard k-epsilon Model. The following two constants are added:

BETA -*Value* is the RNG model constant,

$$\beta_\infty$$

ETAI -*Value* is the asymptotic value of the strain rate parameter eta.

Inlet parameters and wall parameters are the same as the Standard k-epsilon Model.

4. k-epsilon Model due to Shih (NKE)

The k-epsilon Model due to Shih (NKE) features a variable Cm term which helps to reduce the excess normal strain terms in the Standard k-epsilon Model. The NKE model also employs a different dissipation source term than the Standard k-epsilon Model.

The NKE and GIR models are recommended for rotating flows.

The NKE Model is an extension of the Standard k-epsilon Model. Four constants are assigned values. The C2, SCTK, and SCTD constants are assigned values that are separate from the Standard k-epsilon Model. The following constant is added:

C1MX - Value is the maximum allowed value of the C1 constant in the turbulent kinetic energy dissipation rate equation.

Inlet parameters and wall parameters are the same as the Standard k-epsilon Model.

5. Nonlinear Model of Girimaji (GIR)

The Nonlinear Model of Girimaji (GIR) is suggested for cases with secondary vortices in the flow. The GIR and NKE models are recommended for rotating flows.

The GIR Model is an extension of the Standard k-epsilon Model. Seven constants are assigned values. The SCTK, and SCTD constants are assigned values that are separate from the Standard k-epsilon Model. The following five constants are added:

G0 - *Value* is the C_1^0 constant.

G1 - *Value* is the C_1^1 constant.

G2 - *Value* is the C_2 constant.

G3 - *Value* is the C_3 constant.

G4 - *Value* is the C_4 constant.

Inlet parameters and wall parameters are the same as the Standard k-epsilon Model.

6. Shih, Zhu, Lumley Model (SZL)

The SZL Model is simpler than the NKE and GIR models. It produces the lowest level of turbulence. The SZL model is numerically efficient, but in some cases the resulting low effective viscosity has an adverse effect on stability. Generally, if the SZL model does not give satisfactory results, it is recommended that you try the RNG model.

If conditions of large strain exist in the flow field, you may want to try the SZL Model after trying the RNG, NKE or GIR models. If the SZL Model gives significantly different results, it is recommended that you refine the mesh in the regions where the turbulence field is strongly altered.

The SZL Model is an extension of the Standard k-epsilon Model. Five constants are assigned values. The SCTK, and SCTD constants are assigned values that are separate from the Standard k-epsilon Model. The following three constants are added:

SZL1 - *Value* is the numerator constant used in the calculation of Cm. It is the A_{szl1} constant.

SZL2 - *Value* is the denominator constant used in the calculation of Cm. It is the A_{szl2} constant.

SZL3 - *Value* is the strain rate multiplier. It is the A_{szl3} constant.

Inlet parameters and wall parameters are the same as the Standard k-epsilon Model.

APPENDIX 4.1: Milestone for the First Semester of 2 Semester Final Year Project

No.	Detail/ Week	1	2	3	4	5	6	7	8	9	10	11	12	13	14	SW	EW
1	Selection of Project Topic	■	■														
	-Propose Topic																
	-Topic assigned to students																
2	Preliminary Research Work			■	■												
	-Introduction																
	-Objective																
	-List of references/literature																
	-Project planning																
3	Submission of Preliminary Report				●												
4	Project Work					■	■	■	■								
	-Reference/Literature																
	- CFD Simulation																
5	Submission of Progress Report									●							
6	Project work continue									■	■	■	■				
	- CFD Simulation																
7	Submission of Interim Report Final Draft													●			
8	Oral Presentation															●	
9	Submission of Interim Report																●

57

APPENDIX 4.2: Milestone for the Second Semester of 2 Semester Final Year Project

No.	Detail/ Week	1	2	3	4	5	6	7	8	9	10	11	12	13	14	SW	EW
1	Project Work Continue -CFD Simulation		███	███	███												
2	Submission of Progress Report 1				●												
3	Project Work Continue - CFD Simulation					███	███	███	███								
4	Submission of Progress Report 2									●							
5	Project work continue - CFD Simulation									███	███	███	███				
6	Submission of Dissertation Final Draft													●			
7	Oral Presentation															●	
8	Submission of Project Dissertation																●

SW   Study Week

EW   Exam Week

58

APPENDIX 5.1: Governing equation for Volume Of Fluid (VOF) analysis

Discretization of the Equations

The momentum, energy, species transport, and turbulence equations all have the form of a scalar transport equation. There are four types of terms: transient, advection, diffusion, and source. For the purposes of describing the discretization methods, let us refer to the variable considered as φ. The form of the scalar transport equation is:

$$\frac{\partial}{\partial t}\left(\rho C_\phi \phi\right) + \frac{\partial}{\partial x}\left(\rho V_x C_\phi \phi\right) + \frac{\partial}{\partial y}\left(\rho V_y C_\phi \phi\right) + \frac{\partial}{\partial z}\left(\rho V_z C_\phi \phi\right) = \frac{\partial}{\partial x}\left(\Gamma_\phi \frac{\partial \phi}{\partial x}\right) + \frac{\partial}{\partial y}\left(\Gamma_\phi \frac{\partial \phi}{\partial y}\right) + \frac{\partial}{\partial z}\left(\Gamma_\phi \frac{\partial \phi}{\partial z}\right) +$$

where:

C_φ = transient and advection coefficient

Γ_φ = diffusion coefficient

S_φ = source terms

Transport Equation Representation

φ	Meaning	DOF	C_φ	Γ_φ	S_φ
v_x	x-velocity	VX	1	μ_e	$\rho g_x - \partial p/\partial x + R_x$
v_y	y-velocity	VY	1	μ_e	$\rho g_y - \partial p/\partial y + R_y$
v_z	z-velocity	VZ	1	μ_e	$\rho g_z - \partial p/\partial z + R_z$
T	temperature	TEMP	Cp	K	$\mu_t \Phi/\mu - \rho\varepsilon + C_4 \beta\mu_t g_i(\partial T/\partial x_i)\sigma_t$
k	kinematic energy	ENKE	1	μ_t/σ_k	$Q_v + E^k + W^v + \mu\Phi + \partial p/\partial t$

59

ε	dissipation rate	ENDS	1	μ_t/σ_ε	$C_1\mu_t\varepsilon\Phi/k - C_2\rho\varepsilon^2/k + C_1 C_\mu C_3 \beta k g_i (\partial T/\partial x_i)/\sigma_t$
Y_i	species mass fraction	SP01–06	1	$\rho\, Dm_i$	0

The discretization process, therefore, consists of deriving the element matrices to put together the matrix equation:

$$([A_e^{transient}] + [A_e^{advection}] + [A_e^{diffusion}])\{\phi_e\} = \{S_e^\phi\}$$

Transient Term

The first of the element matrix contributions is from the transient term. The general form is simply:

$$[A_e^{transient}] = \int W^e \frac{\partial(\rho C_\phi \phi)^e}{\partial t} d(vol)$$

A lumped mass approximation is used so that

$$\int W^e \frac{\partial(\rho C_\phi \phi)}{\partial t} d(vol) = \frac{\partial(\rho C_\phi \phi)}{\partial t} \int W^e d(vol)$$

For a Volume of Fluid (VOF) analysis, the above equation is modified as only the results at one previous time step are needed:

$$\frac{\partial(\rho\phi)}{\partial t} = \frac{(\rho\phi)_n}{\Delta t} - \frac{(\rho\phi)_{n-1}}{\Delta t}$$

Advection Term

Assume that the advection term,

$$\frac{\partial(\rho C_\phi v_x \phi)}{\partial x} + \frac{\partial(\rho C_\phi v_y \phi)}{\partial y} + \frac{\partial(\rho C_\phi v_z \phi)}{\partial z} = \frac{\partial(\rho C_\phi v_s \phi)}{\partial s}$$

The element-based nodal velocities are made to satisfy the continuity equation, whereas the traditional velocities are made to satisfy the momentum equations.

$$[A_e^{advection}] = \int W^e \left\{ \frac{\partial(\rho v_x^e C_\phi \phi)}{\partial x} + \frac{\partial(\rho v_y^e C_\phi \phi)}{\partial y} + \frac{\partial(\rho v_z^e C_\phi \phi)}{\partial z} \right\} d(vol) +$$

$$C_{2\tau} \int \frac{zh}{2U_{mag}^e} \left\{ \frac{v_x^e \partial W^e}{\partial x} + \frac{v_y^e \partial W^e}{\partial y} + \frac{v_z^e \partial W^e}{\partial z} \right\}$$

$$\left\{ \frac{v_x^e \partial(\rho C_\phi \phi)}{\partial x} + \frac{v_y^e \partial(\rho C_\phi \phi)}{\partial y} + \frac{v_z^e \partial(\rho C_\phi \phi)}{\partial z} \right\} d(vol)$$

In this approach, the pressure equation is derived from the element-based nodal velocities, and it is generally asymmetric even for incompressible flow problems.

Diffusion Terms

The expression for the diffusion terms comes from integration over the problem domain after the multiplication by the weighting function.

$$\text{Diffusion contribution} = \int W^e \frac{\partial}{\partial x}\left(\Gamma_\phi \frac{\partial \phi}{\partial x}\right) d(vol) + \int W^e \frac{\partial}{\partial y}\left(\Gamma_\phi \frac{\partial \phi}{\partial y}\right) d(vol)$$

$$\int W^e \frac{\partial}{\partial z}\left(\Gamma_\phi \frac{\partial \phi}{\partial z}\right) d(vol)$$

61

The x, y and z terms are all treated in similar fashion. Therefore, the illustration is with the term in the x direction. Integration by parts is applied:

$$\int W^e \frac{\partial}{\partial x}\left(\Gamma_\phi \frac{\partial \phi}{\partial x}\right) d(vol) = \int \frac{\partial W^e}{\partial x} \Gamma_\phi \frac{\partial \phi}{\partial x} d(vol)$$
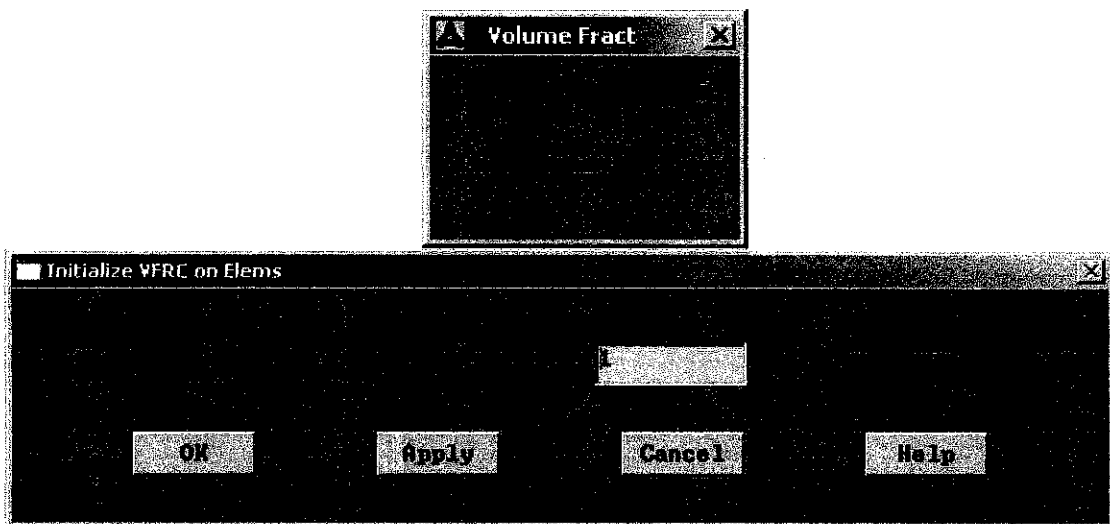
The diffusion matrix may now be expressed as:

$$[A_e^{diffusion}] = \int W_x^e \Gamma_\phi W_x^e + W_y^e \Gamma_\phi W_y^e + W_z^e \Gamma_\phi W_z^e \, d(vol)$$

APPENDIX 5.2: ANSYS GUI for VOF activation
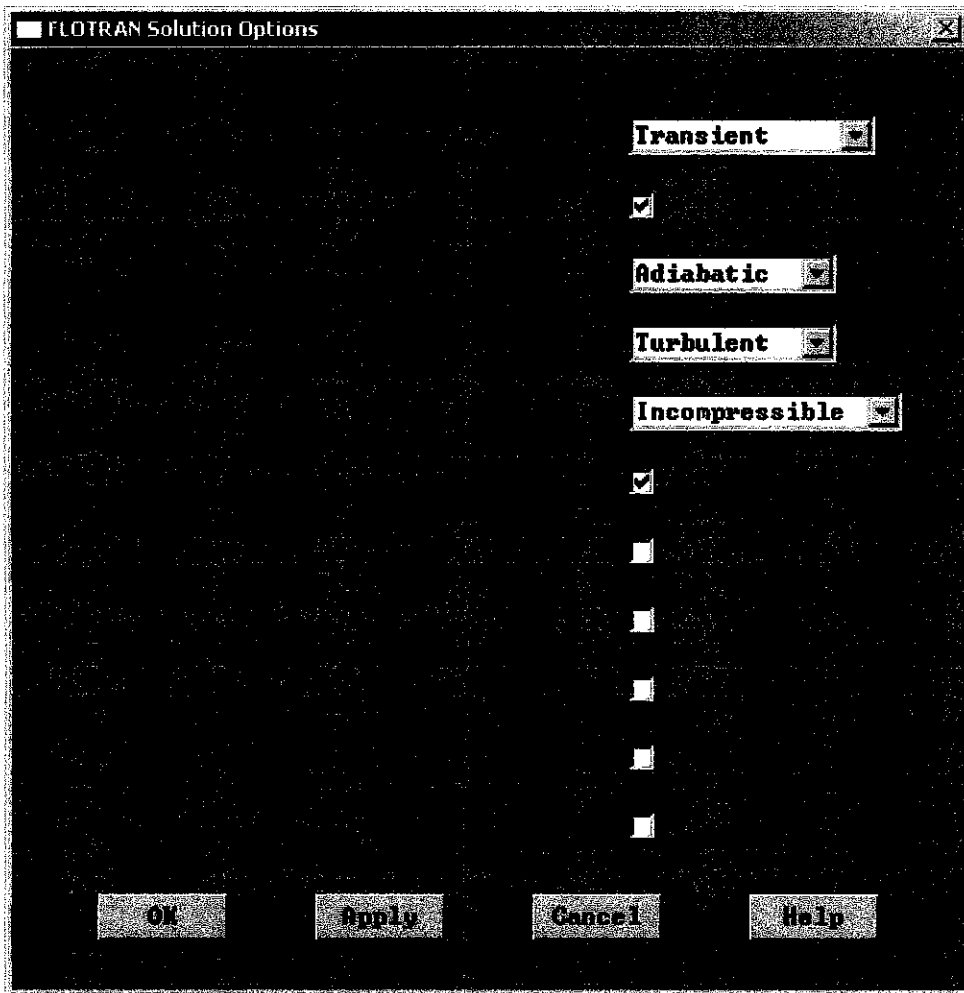
APPENDIX 5.3: ANSYS GUI for initial VFRC load

APPENDIX 5.4: ANSYS GUI for ambient condition
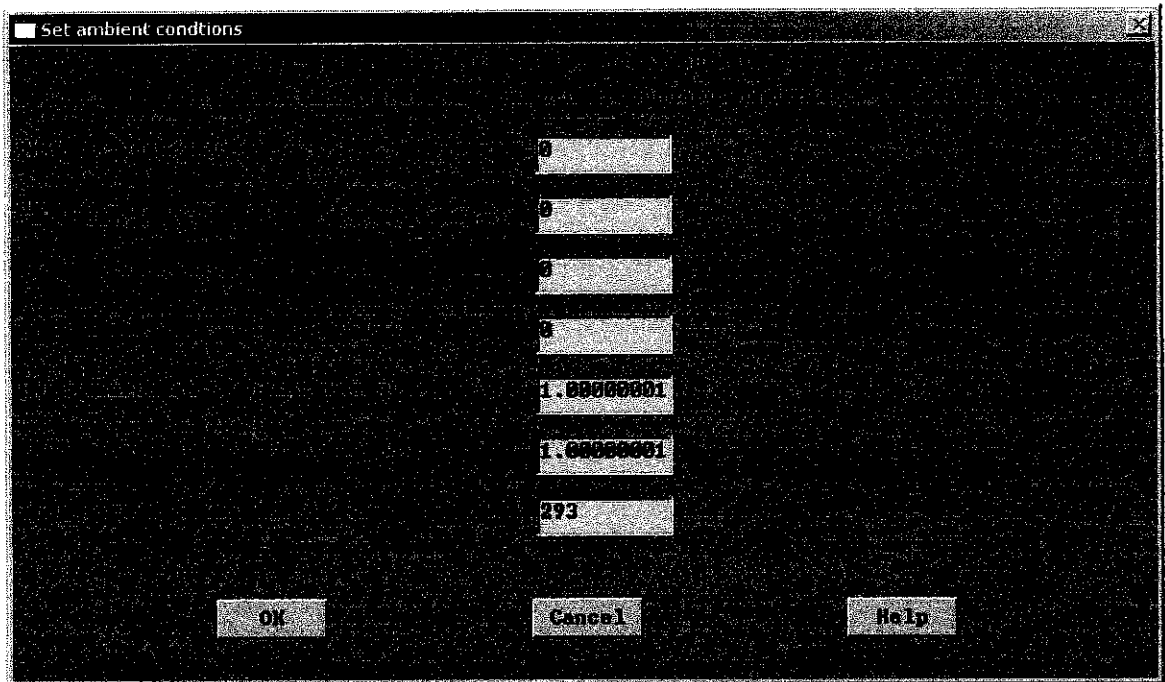
APPENDIX 5.5: ANSYS GUI for VFRC tolerance
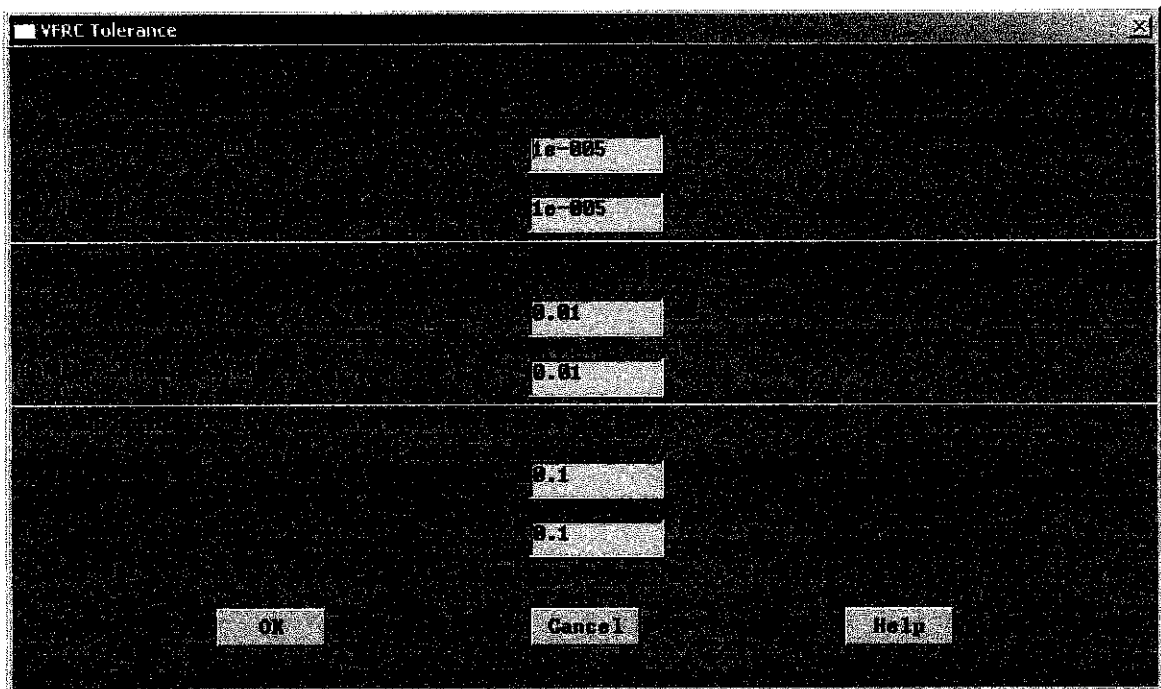
APPENDIX 6.1: Results for different turbulence model
1. Standard k-epsilon Model
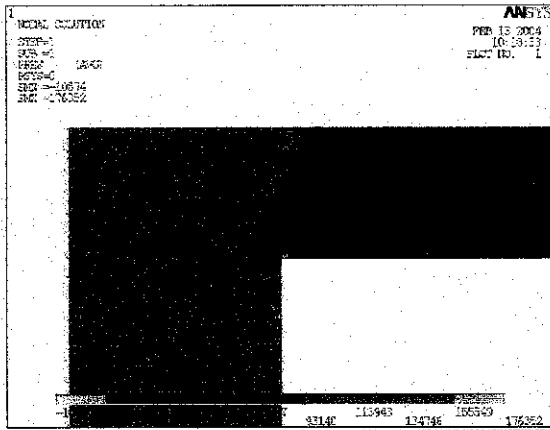
Pressure plot
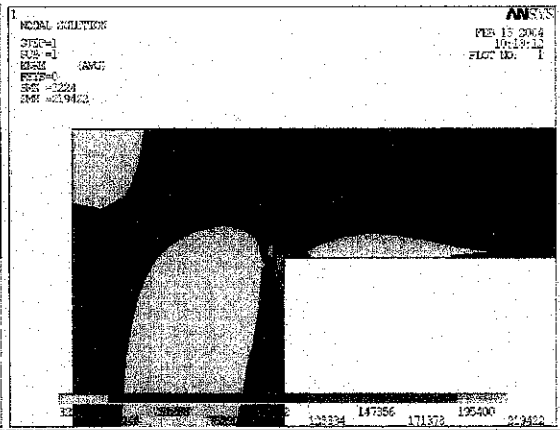
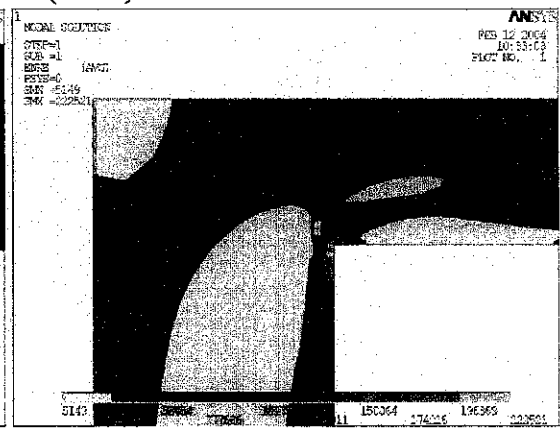Turbulent K.E. plot

2. Equation Turbulence Model (ZeroEq)
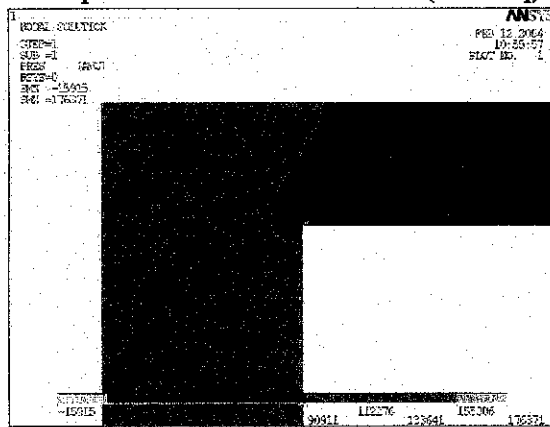
Pressure plot

There is error for **Turbulent K.E. plot**
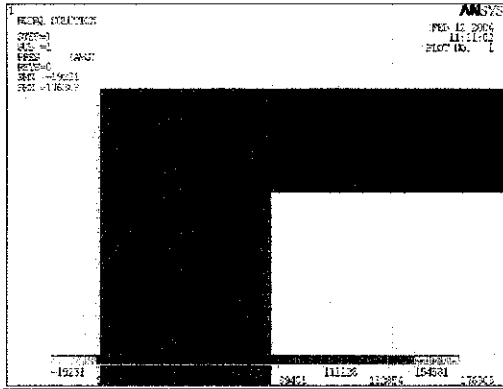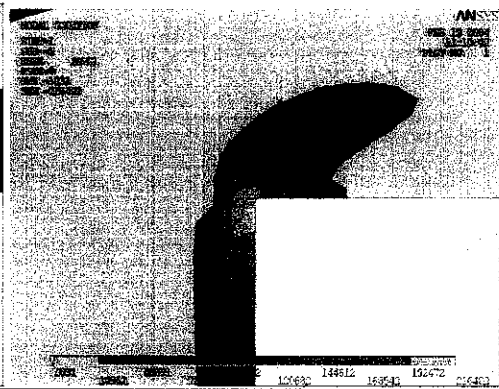
3. Re-Normalized Group Turbulence Model (RNG)
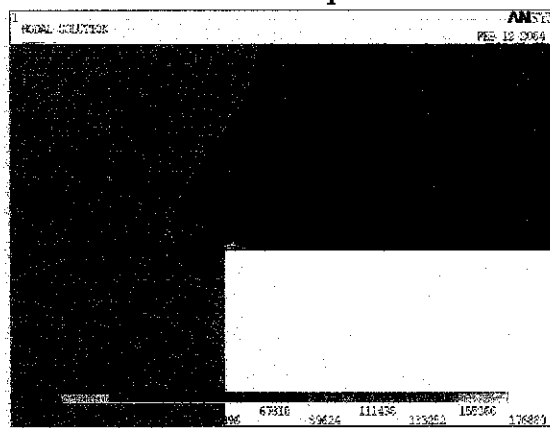
Pressure plot

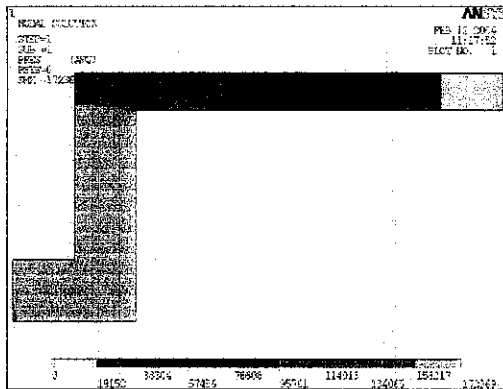

Turbulent K.E. plot

4. k-epsilon Model due to Shih (NKE)

Pressure plot   **Turbulent K.E. plot**

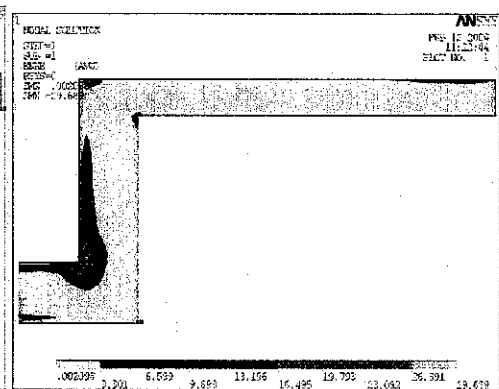## 5. Non-linear Model of Girimaji (GIR)

Pressure plot   **Turbulent K.E. plot**

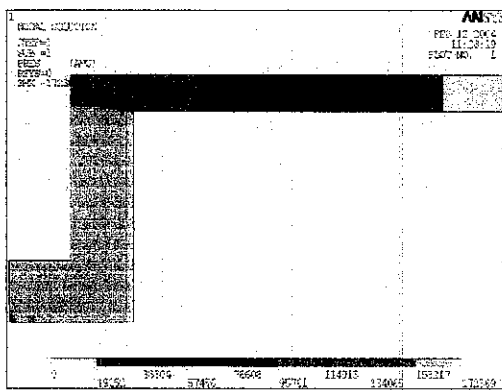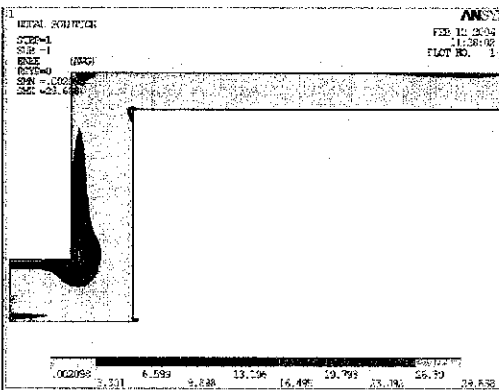## 6. Shih, Zhu, Lumley Model (SZL)

Pressure plot   **Turbulent K.E. plot**

66